

# Modulation of glutamine metabolism by the PI(3)K–PKB–FOXO network regulates autophagy

Kristan E. van der Vos<sup>1,7</sup>, Pernilla Eliasson<sup>2,8</sup>, Tassula Proikas-Cezanne<sup>3,8</sup>, Stephin J. Vervoort<sup>2,6</sup>, Ruben van Boxtel<sup>2</sup>, Marrit Putker<sup>4</sup>, Iris J. van Zutphen<sup>4</sup>, Mario Mauthe<sup>3</sup>, Sebastian Zellmer<sup>5</sup>, Corneliëke Pals<sup>2</sup>, Liesbeth P. Verhagen<sup>2</sup>, Marian J. A. Groot Koerkamp<sup>4</sup>, A. Koen Braat<sup>2,6</sup>, Tobias B. Dansen<sup>4</sup>, Frank C. Holstege<sup>4</sup>, Rolf Gebhardt<sup>5</sup>, Boudewijn M. Burgering<sup>4</sup> and Paul J. Coffey<sup>1,2,6,9</sup>

The PI(3)K–PKB–FOXO signalling network provides a major intracellular hub for the regulation of cell proliferation, survival and stress resistance. Here we report an unexpected role for FOXO transcription factors in regulating autophagy by modulating intracellular glutamine levels. To identify transcriptional targets of this network, we performed global transcriptional analyses after conditional activation of the key components PI(3)K, PKB/Akt, FOXO3 and FOXO4. Using this pathway approach, we identified glutamine synthetase as being transcriptionally regulated by PI(3)K–PKB–FOXO signalling. Conditional activation of FOXO also led to an increased level of glutamine production. FOXO activation resulted in mTOR inhibition by preventing the translocation of mTOR to lysosomal membranes in a glutamine-synthetase-dependent manner. This resulted in an increased level of autophagy as measured by LC3 lipidation, p62 degradation and fluorescent imaging of multiple autophagosomal markers. Inhibition of FOXO3-mediated autophagy increased the level of apoptosis, suggesting that the induction of autophagy by FOXO3-mediated glutamine synthetase expression is important for cellular survival. These findings reveal a growth-factor-responsive network that can directly modulate autophagy through the regulation of glutamine metabolism.

In metazoans, including humans, a plethora of extracellular stimuli activate phosphatidylinositol 3-kinase class I (PI(3)K) and thereby the serine/threonine protein kinase B (PKB, also known as Akt; refs 1,2). The forkhead box (FOX) O transcription factors are directly phosphorylated by PKB, resulting in their nuclear exclusion and transcriptional inactivation (reviewed in ref. 3). The PI(3)K–PKB–FOXO signalling module is evolutionarily conserved, and in the nematode worm *Caenorhabditis elegans* activation of an orthologue of the insulin receptor, DAF-2, results in activation of AGE-1, the *C. elegans* orthologue of PI(3)K, which induces activation of AKT/PKB. Inhibition of this pathway confers stress resistance and *dauer* formation, thereby markedly extending the lifespan of these worms, which is dependent on the FOXO transcription factor DAF-16 (refs 4–6).

In mammals, three FOXO homologues are phosphorylated and regulated by PKB: FOXO1, FOXO3 and FOXO4, which act as transcriptional activators as well as repressors (reviewed in ref. 3). Activation of FOXOs can, depending on the cell type, have an influence

on a wide range of biological processes including cell cycle regulation, stress resistance, development, reproduction and ageing (reviewed in ref. 7). In a manner similar to DAF-16, FOXOs can increase the level of survival of cells during growth-factor deprivation by increasing stress resistance. FOXO activation can protect cells from damage by upregulating the expression of proteins involved in protection against oxidative stress such as manganese superoxide dismutase (MnSOD) and the growth arrest and DNA damage response protein Gadd45, which is involved in DNA repair mechanisms<sup>8,9</sup>. Here we demonstrate an unexpected role for FOXOs in regulating autophagy through modulation of glutamine synthetase activity.

## RESULTS

### PI(3)K–PKB–FOXO signalling regulates glutamine synthetase expression

To globally identify transcriptional targets regulated by PI(3)K–PKB–FOXO signalling, we generated Ba/F3 cell lines, each ectopically

<sup>1</sup>Department of Immunology, University Medical Center Utrecht, Utrecht 3584CX, The Netherlands. <sup>2</sup>Department of Cell Biology, University Medical Center Utrecht, Utrecht 3584CX, The Netherlands. <sup>3</sup>Autophagy Laboratory, Interfaculty Institute for Cell Biology, University of Tuebingen, Tuebingen 72076, Germany. <sup>4</sup>Department of Molecular Cancer Research, University Medical Center, Utrecht 3584CX, The Netherlands. <sup>5</sup>Institut für Biochemie, Medizinische Fakultät, Universität Leipzig, Leipzig 04103, Germany. <sup>6</sup>Center for Molecular and Cellular Intervention, Wilhelmina Children's Hospital, Utrecht 3584EA, The Netherlands. <sup>7</sup>Present address: Departments of Neurology and Radiology, Massachusetts General Hospital, and Neuroscience Program, Harvard Medical School, Boston, Massachusetts 02129, USA. <sup>8</sup>These authors contributed equally to this work.

<sup>9</sup>Correspondence should be addressed to P.J.C. (e-mail: P.J.Coffey@umcutrecht.nl)

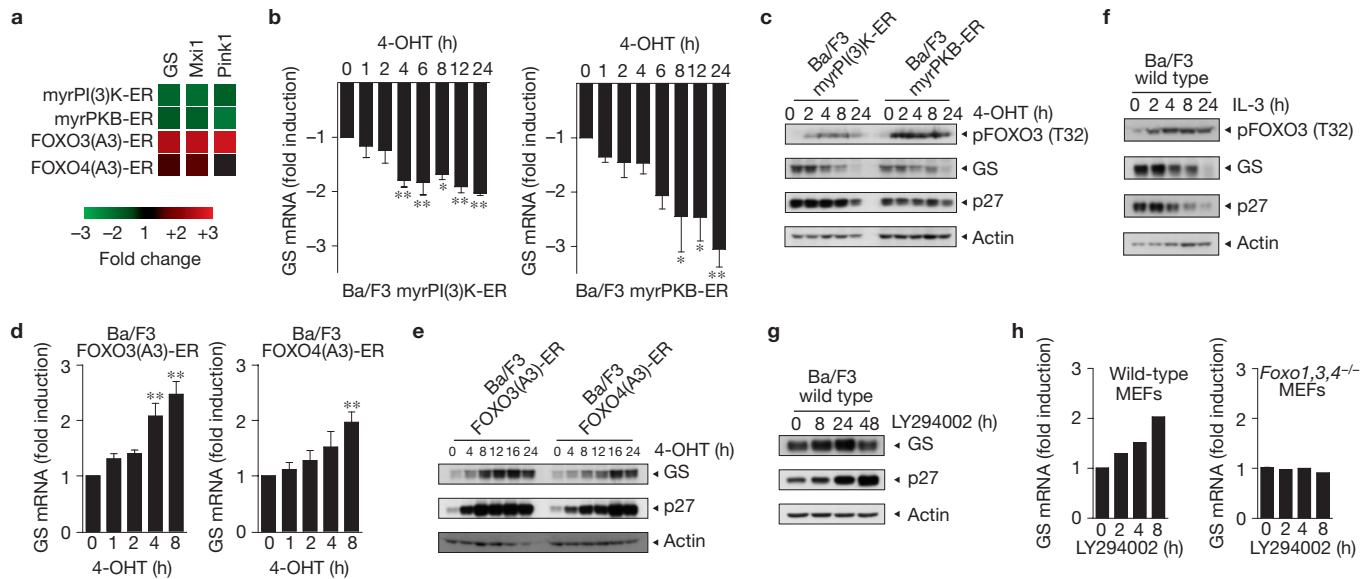


**Figure 1** Modulation of the PI(3)K–PKB–FOXO signalling network results in regulation of glutamine synthetase mRNA and protein levels. **(a)** Ba/F3 cells expressing myrPI(3)K-ER, myrPKB-ER, FOXO3(A3)-ER or FOXO4(A3)-ER were stimulated with 4-OHT for 4 h (myrPI(3)K-ER, myrPKB-ER) or 8 h (FOXO3(A3)-ER and FOXO4(A3)-ER) and microarray analyses were performed. Shown are the fold changes relative to control cells for glutamine synthetase (GS), Mxi1 and Pink1. Data are represented as mean values of one experiment performed in quadruplicate. **(b)** Ba/F3 cells expressing either myrPI(3)K-ER or myrPKB-ER were cytokine starved overnight and stimulated with 4-OHT. Relative mRNA levels of glutamine synthetase were analysed using quantitative rtPCR. Data are represented as mean  $\pm$  s.e.m. normalized for B<sub>2</sub>M ( $n=4$ ). \* $P < 0.05$ , \*\* $P < 0.01$ . **(c)** Ba/F3 cells expressing either myrPI(3)K-ER or myrPKB-ER were cytokine starved overnight and stimulated with 4-OHT. Cell lysates were analysed for protein levels of phospho-FOXO3 (T32), glutamine synthetase, p27 and actin. Shown are representative blots ( $n=4$ ). **(d)** Ba/F3 cells expressing either FOXO3(A3)-ER or FOXO4(A3)-ER were stimulated with 4-OHT in the

presence of mIL-3. Relative mRNA levels of glutamine synthetase were analysed using quantitative rtPCR. Data are represented as mean  $\pm$  s.e.m. values normalized for B<sub>2</sub>M ( $n=3$ ). \*\* $P < 0.01$ . **(e)** Ba/F3 cells expressing either FOXO3(A3)-ER or FOXO4(A3)-ER were stimulated with 4-OHT in the presence of mIL-3. Cell lysates were analysed for protein levels of glutamine synthetase, p27 and actin. Shown are representative blots ( $n=3$ ). **(f)** Wild-type Ba/F3 cells were cytokine starved overnight and stimulated with mIL-3. Cell lysates were analysed for protein levels of phospho-FOXO3 (T32), glutamine synthetase, p27 and actin. Shown are representative blots ( $n=4$ ). **(g)** Wild-type Ba/F3 cells were incubated with LY294002 in the presence of mIL-3. Cell lysates were analysed for protein levels of glutamine synthetase, p27 and actin. Shown are representative blots ( $n=3$ ). **(h)** FOXO1,3,4<sup>-/-</sup> MEFs and wild-type MEFs were incubated with LY294002 (10  $\mu$ M) for the indicated times. Cell RNA was isolated and relative mRNA levels of glutamine synthetase were analysed using quantitative PCR. Data are represented as mean values normalized for B<sub>2</sub>M ( $n=2$ ). Uncropped images of blots are shown in Supplementary Fig. S7.

expressing conditionally active variants of the three key components in this pathway. To selectively activate these proteins, myrPI(3)K, myrPKB, FOXO3(A3) or FOXO4(A3) were fused to the hormone-binding domain of the oestrogen receptor (ER), thereby rendering them inducible by 4-hydroxytamoxifen (4-OHT). We subsequently performed microarray analyses after activation of each pathway component (<http://www.ncbi.nlm.nih.gov/geo/>, accession number: GSE35705). To identify specific pathway targets, we focused on changes in messenger RNA transcripts that were downregulated by both PI(3)K and PKB activation, and upregulated by FOXO3 and FOXO4 or vice versa. Among the identified transcriptional targets we found Mxi1 and Pink1, both recently described to be regulated by PI(3)K–PKB–FOXOs, validating this approach<sup>10,11</sup> (Fig. 1a).

Using this stringent pathway analysis we identified glutamine synthetase as a transcriptional target (Fig. 1a). Evaluating glutamine synthetase mRNA and protein levels in the various cell lines by quantitative real-time PCR (rtPCR) and in parallel western blotting confirmed that glutamine synthetase is upregulated by both FOXO3 and FOXO4 activation, whereas activation of either PI(3)K or PKB inhibits its expression (Fig. 1b–e). We next evaluated whether activation or inhibition of endogenous PI(3)K signalling resulted in a similar modulation of the glutamine synthetase protein levels. Stimulation of cells with interleukin

(IL)-3 also resulted in a reduction in the level of glutamine synthetase protein expression, correlating with FOXO inhibition (Fig. 1f). Furthermore, inhibition of PI(3)K activity utilizing the specific inhibitor LY294002 was able to recapitulate the effects observed after 4-OHT-induced FOXO activation (Fig. 1g). Treatment of wild-type mouse embryonic fibroblasts (MEFs) or FOXO1,3,4 triple-knockout (TKO) MEFs with LY294002 further demonstrated that FOXOs were necessary for upregulation of glutamine synthetase mRNA levels (Fig. 1h).

Actinomycin D abrogated FOXO3-induced glutamine synthetase upregulation, demonstrating that this was a direct transcriptional response (Fig. 2a). Co-transfection of FOXO3(A3) with glutamine synthetase promoter luciferase reporter constructs identified a FOXO-responsive enhancer of 384 base pairs (bp) between  $-2,520/-2,146$  bp (Supplementary Fig. S1a,b). Alignment of the identified 384-bp fragment from human, mouse and rat glutamine synthetase promoters shows the presence of five conserved FOXO binding sites (Supplementary Fig. S1c). Mutational analysis revealed that FOXO-induced reporter activity was dependent on the presence of FOXO binding site 2 (Fig. 2b). To demonstrate that FOXO3 directly binds at this site *in vivo*, cells were treated with the PI(3)K inhibitor LY294002 and chromatin immunoprecipitation assays were performed. Quantitative rtPCR analysis of promoter fragments isolated by FOXO3 immunoprecipitation demonstrated

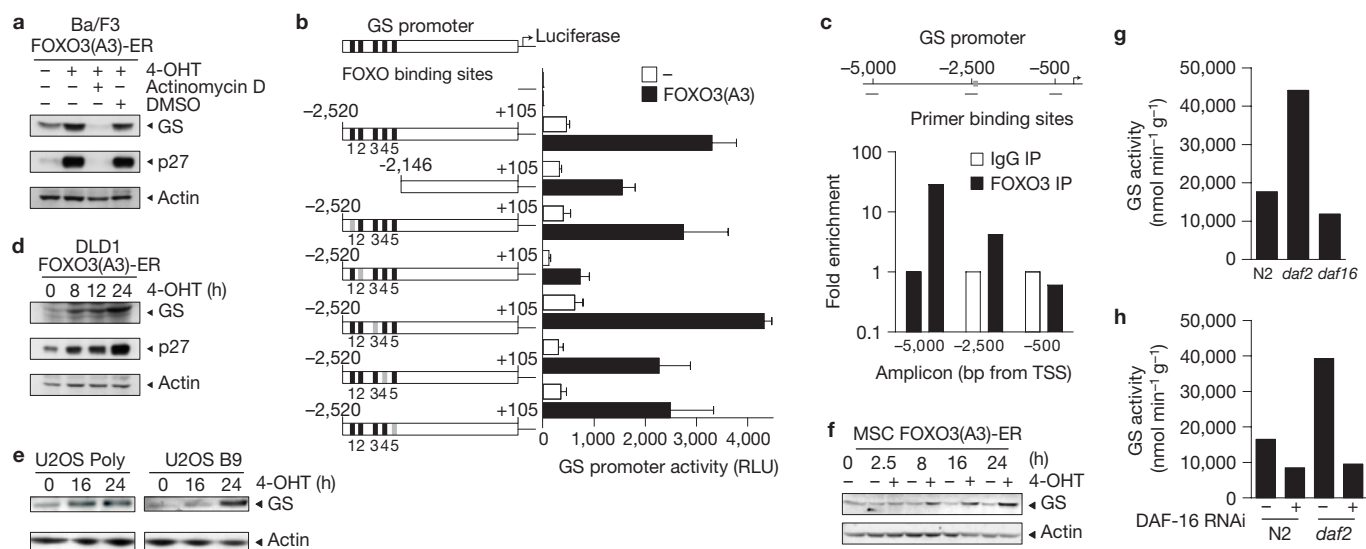


**Figure 2** FOXO-mediated regulation of glutamine synthetase expression is transcriptionally regulated and evolutionarily conserved. **(a)** Ba/F3 cells expressing FOXO3(A3)-ER were stimulated with 4-OHT and actinomycin D ( $1 \mu\text{g ml}^{-1}$ ) or dimethylsulphoxide (DMSO) as a control in the presence of mIL-3 for 16 h. Cell lysates were analysed for protein levels of glutamine synthetase (GS), p27 and actin. Shown are representative blots ( $n = 3$ ). **(b)** Glutamine synthetase reporter plasmids carrying mutations in putative FOXO-binding sites were transfected in HEK293 cells together with Renilla and FOXO3(A3) as indicated. Luciferase activity was measured 40 h after transfection. Data are depicted as relative luciferase units (RLU) compared with the control. Shown are mean  $\pm$  s.e.m. values ( $n = 3$ ). **(c)** HEK293 cells were stimulated with LY294002 for 24 h and chromatin immunoprecipitations were performed. Protein–DNA complexes were formaldehyde-crosslinked, and chromatin fragments from these cells were subjected to immunoprecipitation with a control antibody or antibodies against FOXO3a, as indicated. After crosslink reversal, the co-immunoprecipitated DNA was amplified by rtPCR. Shown are the means of duplicates within one experiment. IP, immunoprecipitate; TSS, transcription start site. **(d)** DLD1 cells expressing FOXO3(A3)-ER were stimulated with 4-OHT. Cell lysates were analysed for protein levels of glutamine synthetase, p27 and actin. Shown are representative blots ( $n = 4$ ). **(e)** The osteosarcoma cell line U2OS expressing FOXO3(A3)-ER was stimulated with 4-OHT, cells were lysed and equal amounts of proteins were analysed for levels of glutamine synthetase and actin. Shown are representative blots ( $n = 3$ ). **(f)** MSCs expressing FOXO3(A3)-ER were stimulated with 4-OHT, cells were lysed and equal amounts of proteins were analysed for levels of glutamine synthetase and actin. Shown are representative blots ( $n = 3$ ). **(g)** Wild-type, *daf-2* and *daf-16* mutant worms were synchronized to L1 by hypochlorite treatment and were placed on nematode growth medium agar plates. After five days worms were lysed in imidazole and analysed for glutamine synthetase activity. **(h)** Wild-type N2 worms or *daf-2* mutants were synchronized to L1 by hypochlorite treatment and placed on nematode growth medium plates with or without bacteria expressing DAF-16 double-stranded RNA. After five days worms were lysed in imidazole and analysed for glutamine synthetase activity. **(g,h)** Shown are the means of five independent plates for each condition. Uncropped images of blots are shown in Supplementary Fig. S7.

that FOXO3 associated with the region previously identified in the glutamine synthetase promoter at  $-2,500$  (Fig. 2c and Supplementary Fig. S1d). We also identified a second binding site for FOXO3, further upstream in the glutamine synthetase promoter ( $-5,000$ ).

The effects mediated by FOXO transcription factors are known to be dependent on cell type<sup>12</sup>. To determine whether regulation of glutamine synthetase expression by FOXO transcription factors was a general phenomenon, we examined glutamine synthetase expression in multiple cell types, including the human colon carcinoma cell line DLD1, the osteosarcoma cell line U2OS and primary human mesenchymal stromal cells (MSCs). Conditional activation of FOXO3 in these disparate cell types again resulted in upregulation of glutamine synthetase protein levels (Fig. 2d–f; see also Fig. 5c). As the PI(3)K–PKB–FOXO module is conserved in most eukaryotes, we wished to determine whether glutamine synthetase regulation might also be evolutionarily conserved. We evaluated glutamine synthetase activity in *C. elegans*, comparing wild-type, *daf-2* (insulin/IGF-1-like receptor) and *daf-16* (FOXO) mutants. The level of glutamine synthetase activity was significantly increased in *daf-2* mutant worms when compared with wild-type worms, whereas *daf-16* mutants showed a lower level of glutamine synthetase activity when compared with wild-type worms (Fig. 2g). RNA-interference-mediated *daf-16* knockdown

completely abrogated the *daf-2*-mediated increase in the level of glutamine synthetase activity (Fig. 2h), providing evidence that FOXO-mediated glutamine synthetase regulation is evolutionarily conserved.

### FOXO3-mediated upregulation of glutamine synthetase expression is accompanied by increased glutamine levels

Glutamine synthetase converts glutamate to glutamine, a process that requires ammonia and ATP (ref. 13). To determine whether the observed FOXO-induced glutamine synthetase upregulation also results in a higher level of glutamine synthetase activity, FOXO3 activity was induced and the level of glutamine synthetase activity in cell lysates was determined. Activation of FOXO3 resulted in an up to fourfold increase in the level of glutamine synthetase activity, correlating with its expression levels (Fig. 3a). Pre-treatment of cells with L-methionine sulphoximine (MSO), an irreversible inhibitor of glutamine synthetase activity<sup>14</sup>, completely abrogated the FOXO3-induced increased level of glutamine synthetase activity, whereas glutamine synthetase expression levels were unaffected (Fig. 3b).

Next, we examined the levels of individual amino acids after conditional activation of PI(3)K, PKB or FOXO3. In cells in which PI(3)K or PKB activity was induced, the glutamine levels were specifically decreased when compared with control cells, whereas

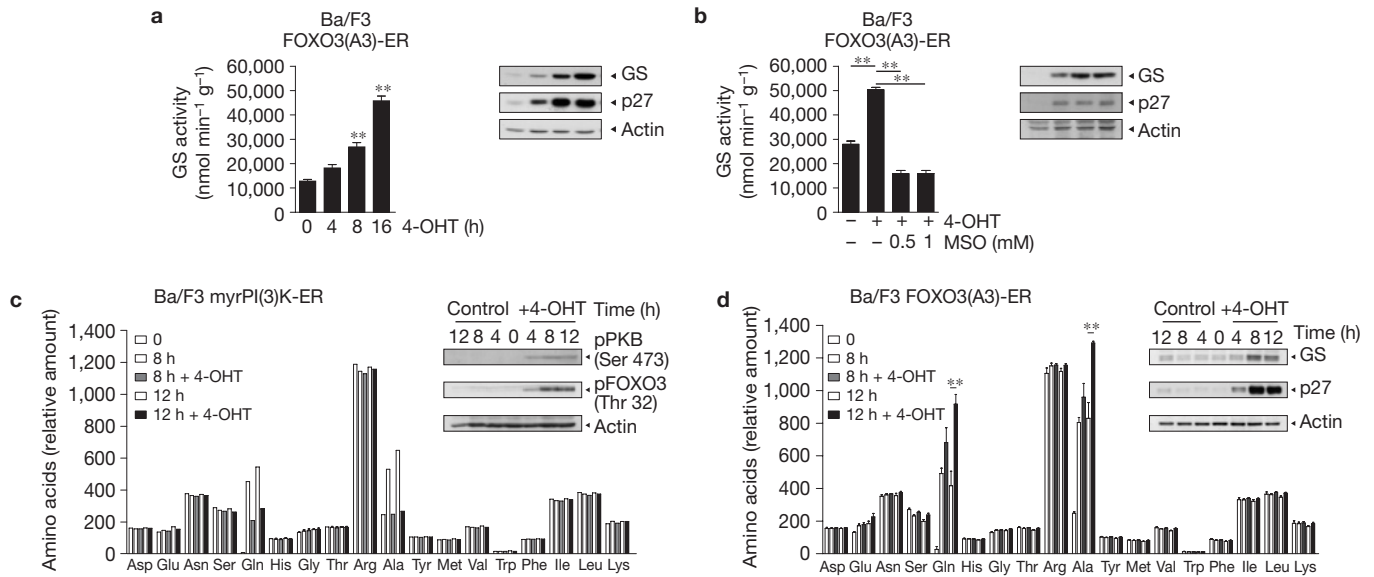


**Figure 3** Modulation of the PI(3)K-PKB-FOXO pathway results in specific regulation of glutamine levels. **(a)** Ba/F3 cells expressing FOXO3(A3)-ER were stimulated with 4-OHT in the presence of mIL-3. Cell lysates were analysed for glutamine synthetase (GS) activity in an enzyme assay (left). In addition, the expression of glutamine synthetase, p27 and actin was determined using western blot (right). Shown are the mean  $\pm$  s.e.m. ( $n=3$ ) and representative blots of these experiments.  $**P < 0.01$ . **(b)** Ba/F3 cells expressing FOXO3(A3)-ER were stimulated with 4-OHT for 16 h in the presence of mIL-3 together with MSO, as indicated. Cell lysates were analysed for glutamine synthetase activity in an enzyme assay (left). Furthermore the expression levels of glutamine synthetase, p27 and actin were determined using western blot (right). Shown are the mean  $\pm$  s.e.m. ( $n=3$ ) and representative blots of these experiments.  $*P < 0.05$ ,  $**P < 0.01$ . **(c)** Ba/F3 cells expressing myrPI(3)K-ER were cytokine-starved overnight.

The next day, cells were washed in PBS and put in a medium without serum, with or without 4-OHT. At the times indicated, medium samples were taken and analysed for amino acid levels by high-performance liquid chromatography. Cells were lysed and equal amounts of protein were analysed by western blotting for levels of phospho-PKB (S473), phospho-FOXO3 (T32) and actin (inset). Shown are the mean of relative amino acid levels, compared with  $t=0$  ( $n=2$ ), and representative blots of these experiments. **(d)** Ba/F3 cells expressing FOXO3(A3)-ER were stimulated with 4-OHT in serum-free medium containing mIL-3. The medium was analysed for amino acid levels by high-performance liquid chromatography. Cells were lysed and analysed for protein levels of glutamine synthetase, p27 and actin (inset). Shown are the mean  $\pm$  s.e.m. of relative amino acid levels, compared with  $t=0$  ( $n=4$ ), and representative blots of these experiments.  $**P < 0.01$ . Uncropped images of blots are shown in Supplementary Fig. S7.

the concentrations of most amino acids were in general unaffected (Fig. 3c and Supplementary Fig. S2). Moreover, conditional activation of FOXO3 resulted specifically in an increase in glutamine levels, correlating with expression of glutamine synthetase (Fig. 3d). Alanine levels were also increased after FOXO3 activation. However, as cells are capable of converting glutamine to alanine, the increased alanine levels are probably a secondary effect of the rise in glutamine levels<sup>15</sup>.

### FOXO3-induced glutamine synthetase expression leads to inhibition of mTOR and increased autophagy

Amino acids play an important role in the regulation of a variety of cellular processes, including proliferation and cell growth, through the control of the mammalian target of rapamycin (mTOR; reviewed in ref. 16). To determine the functional consequences of PI(3)K-PKB-FOXO-mediated regulation of glutamine metabolism, FOXO3 was activated for 24 h, and cells were subsequently briefly starved and then re-stimulated with essential amino acids (EAAs). EAA stimulation was sufficient to increase the level of phosphorylation of the mTOR substrate p70S6 kinase (S6K; Fig. 4a, lane 2), which was mTOR dependent because pre-treatment with the mTOR inhibitor rapamycin completely blocked this (lane 6). In cells in which FOXO3 had been activated, amino-acid re-feeding resulted in a reduced level of p70S6 kinase phosphorylation (lane 4). This decrease in the level of phosphorylation was dependent on glutamine synthetase because FOXO3 activation in the presence of MSO rescued the inhibition of

S6K phosphorylation (lane 8), supporting the fact that FOXO3 inhibits mTOR activity through glutamine synthetase.

Recent studies have shown that in response to amino acids mTORC1 is targeted to the cytoplasmic face of lysosomes, a process that is required for its activation by RheB (ref. 17). In control cells we observed that mTOR was localized in distinct spots that co-localized with the lysosomal marker LAMP2 (Fig. 4b,c). FOXO3 activation resulted in a more diffuse cytoplasmic staining of mTOR disrupting co-localization with LAMP2, whereas cells incubated with both 4-OHT and MSO showed co-localization similar to the control cells. These results suggest that the FOXO3-induced glutamine synthetase activity inhibits mTOR activation by blocking the translocation of mTOR to the lysosomal surface.

The activity of mTOR plays an evolutionarily conserved role in the negative regulation of autophagy<sup>18,19</sup>. Autophagy can be measured by analysing autophagosome-bound lipidated LC3 (LC3-II) protein<sup>20</sup>. After FOXO3 activation the level of LC3-II protein was strongly increased (Fig. 4d). Importantly, MSO treatment blocked the FOXO-induced increase in LC3-II, demonstrating that LC3 lipidation is dependent on glutamine synthetase activity (Fig. 4d). These observations were further validated through the use of a glutamine-synthetase-targeted short interfering RNA (siRNA) that also reduced FOXO-mediated LC3-II formation (Fig. 4e) and reduced the degradation of the autophagy marker p62 (Fig. 4f and Supplementary Fig. S3a). To determine whether FOXO3 activation not only increases lipidation of LC3, but also permits subsequent degradation of

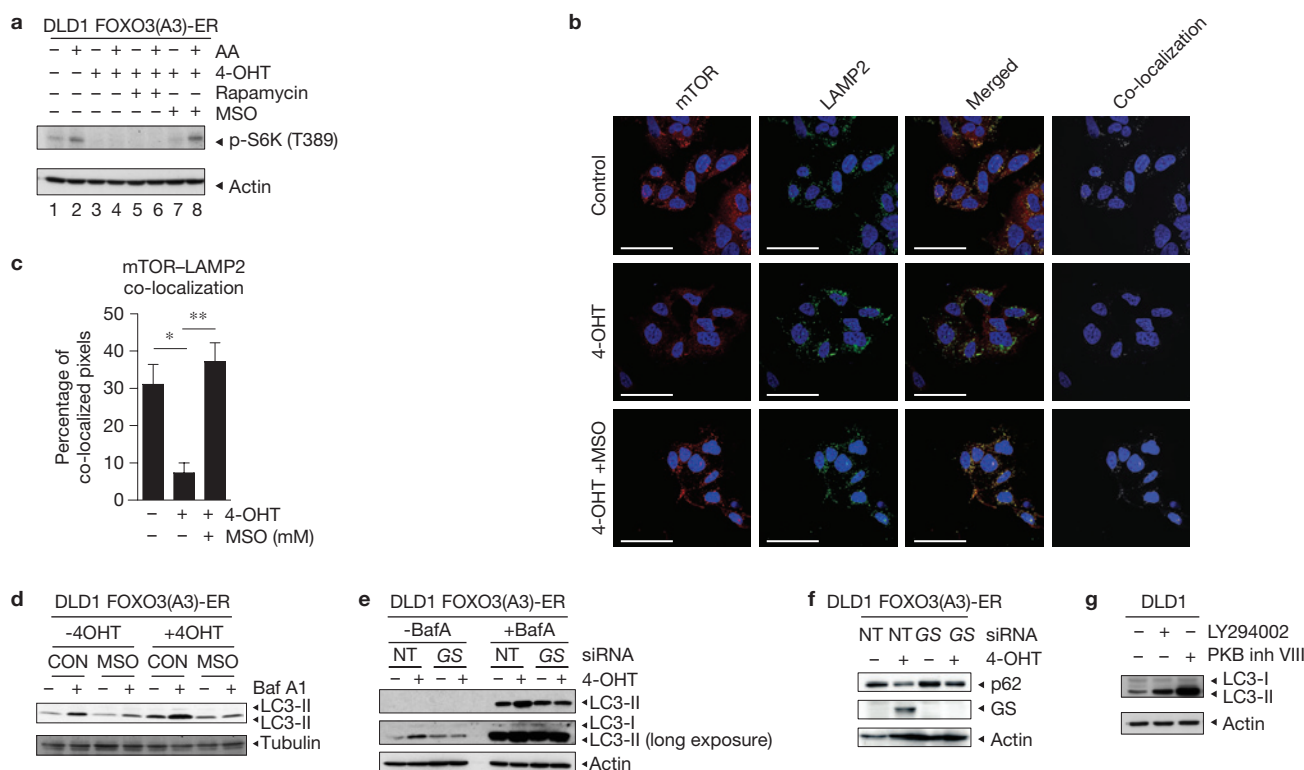


**Figure 4** Regulation of glutamine synthetase expression by PI(3)K-PKB-FOXO inhibits mTOR and modulates autophagy. **(a)** DLD1 cells expressing FOXO3(A3)-ER were stimulated with 4-OHT with or without MSO. After 24 h, the cells were starved of serum, amino acids and glucose in D-PBS containing the indicated inhibitors and stimulated with amino acids for 10 min. Cell lysates were analysed for protein levels of phospho-S6K (Thr 389) and actin. Shown are representative blots of three independent experiments. **(b,c)** DLD1 cells expressing FOXO3(A3)-ER were stimulated with 4-OHT and MSO (0.25 M) for 24 h in glutamine-free DMEM containing 0.1% FCS. Cells were stained for mTOR and LAMP2 and analysed by confocal microscopy. **(b)** Shown are representative pictures ( $n=4$ ). Scale bars, 100  $\mu\text{m}$ . **(c)** Quantification of co-localization between mTOR and LAMP2 as seen in **b**. Depicted are the mean  $\pm$  s.e.m. of the percentage of co-localized pixels from four experiments. \* $P < 0.05$ , \*\* $P < 0.01$ . **(d)** DLD1 cells expressing FOXO3(A3)-ER were treated with

or without 4-OHT, MSO and BafA1 (200 nM). After 24 h, cell lysates were analysed for protein levels of LC3 and tubulin. Shown are representative blots ( $n=4$ ). **(e)** DLD1 cells expressing FOXO3(A3)-ER were transfected with glutamine synthetase (GS) siRNA or a non-targeting siRNA and stimulated with 4-OHT in glutamine-free DMEM containing 0.1% FBS. After 24 h, cell lysates were analysed for protein levels of glutamine synthetase, LC3 and actin. Shown are representative blots ( $n=2$ ). **(f)** DLD1 cells expressing FOXO3(A3)-ER were transfected with glutamine synthetase siRNA or non-template (NT) control siRNA and stimulated with 4-OHT for 16 h. Cells were lysed and equal amounts of proteins were analysed for levels of p62 or glutamine synthetase. Shown are representative blots ( $n=2$ ). **(g)** DLD1 cells were stimulated with LY294002 or PKB inhibitor VIII for 24 h. Cell lysates were analysed for protein levels of LC3 and actin. Shown are representative blots ( $n=4$ ). Uncropped images of blots are shown in Supplementary Figs S7 and S8.

autophagosomal content, cells were treated with the lysosomal inhibitor bafilomycin A (BafA1). Under such conditions a further increase of LC3-II protein abundance indicates the induction of the complete process of autophagy<sup>21</sup>. The addition of BafA1 further increased FOXO3-induced LC3 lipidation, demonstrating that FOXO3 activation induces autophagic flux through both the formation and degradation of autophagosomes (Fig. 4d,e and Supplementary Fig. S3b).

To evaluate the effect of modulating endogenous FOXO activity, cells were treated with either LY294002 or PKB inhibitor VIII. Both treatments again resulted in increased LC3-II levels (Fig. 4g and Supplementary Fig. S3c,d). Next, we analysed the number of autophagosomes in FOXO3-activated cells by visualizing LC3 by immunofluorescent imaging (Fig. 5a,b and Supplementary Fig. S3e). In control cells LC3 showed a diffuse cytoplasmic distribution; however, FOXO3 activation showed distinct LC3-positive punctate spots. Importantly, treating cells with 4-OHT in the presence of MSO abrogated the increase in the numbers of LC3-positive autophagosomes, demonstrating the necessity for glutamine synthetase activity.

Furthermore, autophagy was analysed in other cell lines. Activation of FOXO3 in MSCs increased the glutamine synthetase expression level, lowered the level of phosphorylation of pS6 and increased the level of lipidation of LC3 (Fig. 5c). The addition of BafA1 further increased the LC3 lipidation level, indicating again that FOXO3-induced glutamine synthetase expression induces autophagy and increases autophagic degradation. In addition, activation of FOXO3 in U2OS cells also increased LC3-II levels (Supplementary Fig. S3f). To evaluate whether endogenous FOXO3 was also capable of inducing autophagy, IL-3 was withdrawn from Ba/F3 cells. Growth-factor-starved cells showed a clear induction of both glutamine synthetase expression and LC3 lipidation, which was further enhanced in the presence of BafA1 (Fig. 5d).

Furthermore, we wished to determine whether increased glutamine levels were sufficient to induce autophagy. Incubating cells with glutamine increased the level of LC3-II protein and blocked phosphorylation of S6K at concentrations as low as 2.5 mM (Fig. 5e). Furthermore, incubating cells with glutamine inhibited starvation-induced mTOR/LAMP2 co-localization (Fig. 5f). These

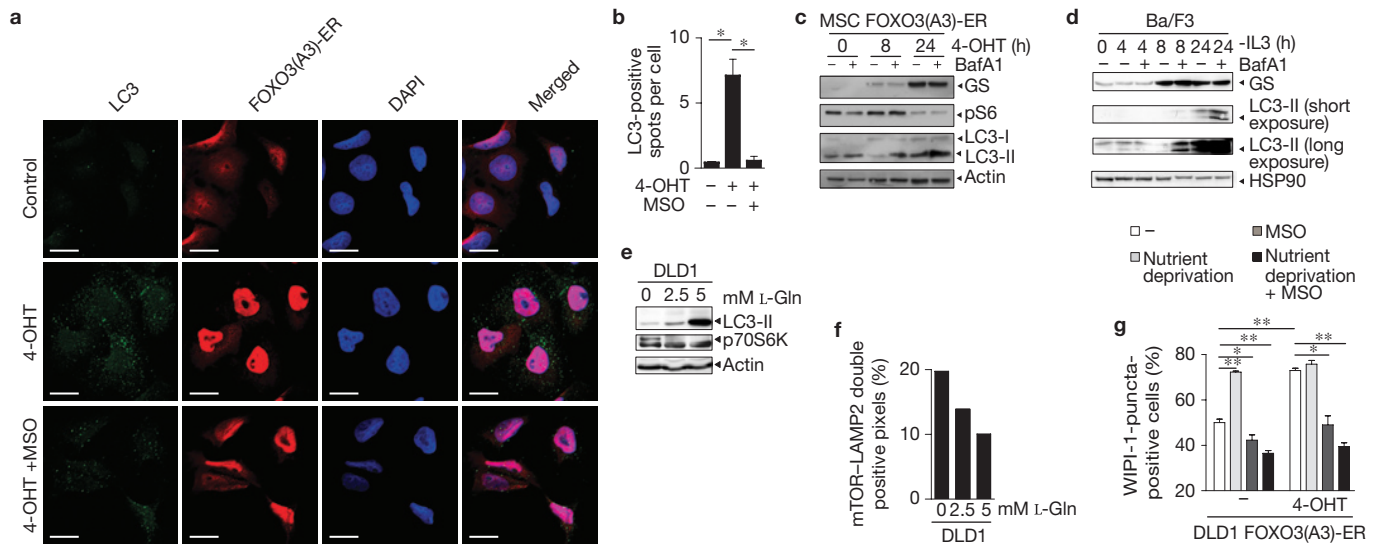


**Figure 5** FOXO-induced glutamine synthetase expression increases the level of autophagy. **(a)** DLD1 cells expressing FOXO3(A3)-ER were stimulated with 4-OHT and MSO for 24 h in glutamine-free DMEM containing 0.1% FCS. Cells were stained for LC3 and ER and analysed by confocal microscopy. Shown are representative pictures ( $n = 3$ ). Scale bars, 20  $\mu\text{m}$ . **(b)** Quantification of LC3-positive spots as seen in **a** using ImageJ software. Depicted are mean  $\pm$  s.e.m. of the number of LC3-positive spots divided by the number of DAPI-positive cells ( $n = 4$ ).  $*P < 0.05$ . **(c)** MSCs expressing FOXO3(A3)-ER were treated with or without 4-OHT and BafA1 (100 nM). At the indicated time points, cell lysates were analysed for protein levels of glutamine synthetase (GS), LC3, pS6 (Ser 235/236) and actin. Shown are representative blots ( $n = 2$ ). **(d)** IL-3 was withdrawn from Ba/F3 cells in the presence or absence of BafA1 (100 nM) as indicated. Cell lysates were analysed for protein levels of glutamine synthetase, LC3 and hsp90. Shown are representative blots ( $n = 2$ ). **(e)** DLD1 cells were stimulated

with L-glutamine (L-Gln) in glutamine-free DMEM containing 0.1% FBS. After 24 h, cell lysates were analysed for protein levels of LC3, p62, p-S6K (Thr 389) and actin. Shown are representative blots ( $n = 3$ ). **(f)** DLD1 cells were starved and stimulated with glutamine (5 and 10 mM). Cells were stained for mTOR and LAMP2 and analysed by confocal microscopy, and the co-localization between mTOR and LAMP2 was quantified by ImageJ. Depicted are the means of the percentage of co-localized pixels ( $n = 2$ ). **(g)** DLD1 cells expressing FOXO3(A3)-ER were transiently transfected with GFP-WIPI-1 and subsequently stimulated with 4-OHT in the presence or absence of MSO in glutamine-free DMEM containing 0.1% FCS or medium without amino acids for 24 h. GFP-WIPI-1 puncta formation analysis was performed by confocal microscopy. Depicted are the percentages of cells positive for GFP-WIPI-1 puncta. Shown are the mean  $\pm$  s.e.m. ( $n = 4$ ).  $*P < 0.05$  and  $**P < 0.01$ . Uncropped images of blots are shown in Supplementary Fig. S8.

data support our previous observations demonstrating that regulation of glutamine levels by glutamine synthetase can modulate mTOR activity and regulate autophagy (Fig. 4).

### FOXO3 induces multiple steps in autophagosome formation through increased glutamine synthetase activity

To further resolve the mechanism of FOXO3-regulated autophagy, we transfected cells expressing FOXO3(A3)-ER with GFP-WIPI-1 and quantified the number of cells exhibiting GFP-WIPI-1 puncta<sup>22</sup>. The percentage of cells positive for WIPI-1 puncta was increased after activation of FOXO3, and this was abolished by MSO (Fig. 5g and Supplementary Fig. S3g). Furthermore, nutrient-deprivation-induced GFP-WIPI-1 puncta formation was also inhibited by MSO, suggesting that both basal and starvation-induced autophagy are critically regulated by the level of glutamine synthesis. These results were further validated through the use of a glutamine-synthetase-targeted siRNA that also reduced FOXO-mediated WIPI puncta formation (Supplementary Fig. S3h). This indicates that FOXO3-mediated autophagy involves the inhibition of mTORC1, the subsequent activation of WIPI-1 upstream of both Atg12 and LC3, and hence canonical, evolutionarily conserved autophagy<sup>23</sup>.

Next, we extended our results to co-localization studies of Atg proteins (reviewed in ref. 24). As shown in Fig. 6a FOXO3 activation increased the level of co-localization of LC3 and ULK2 (Atg1 homologue), which was abolished on MSO treatment. Furthermore,

FOXO3-induced glutamine synthetase expression also resulted in an increased level of co-localization of WIPI-1 with p62 or Atg12 (Fig. 6b,c and Supplementary Fig. S4a). Importantly, the addition of glutamine to cells treated with 4-OHT and MSO reversed the MSO-mediated inhibition of FOXO3-induced p62 puncta (Supplementary Fig. S4b), indicating that the inhibition of autophagy observed with the glutamine synthetase inhibitor MSO is glutamine synthetase specific. Fluorescent imaging therefore shows that FOXO3 modulates multiple steps in the autophagic cascade through an increased level of glutamine synthetase activity resulting in autophagosome formation.

### Induction of autophagy by glutamine synthetase increases cell survival

The induction of autophagy is an important cell survival mechanism under conditions of nutrient or growth-factor starvation, and inhibition of autophagic flux can result in an increased level of cell death<sup>25</sup>. We investigated autophagy and cell death in Foxo1,3,4 TKO MEFs. Wild-type MEFs or TKO MEFs were serum starved in the absence or presence of BafA1 or chloroquine, both inhibitors of autophagic flux<sup>26</sup>. LC3-II levels in TKO MEFs were lower than in wild-type MEFs, further supporting a role for FOXO transcription factors in regulating autophagy (Supplementary Fig. S4c). Furthermore, inhibition of autophagy in wild-type MEFs resulted in significantly increased levels of apoptosis (Supplementary Fig. S4d). In contrast, no increase in apoptosis was observed after inhibition of autophagy

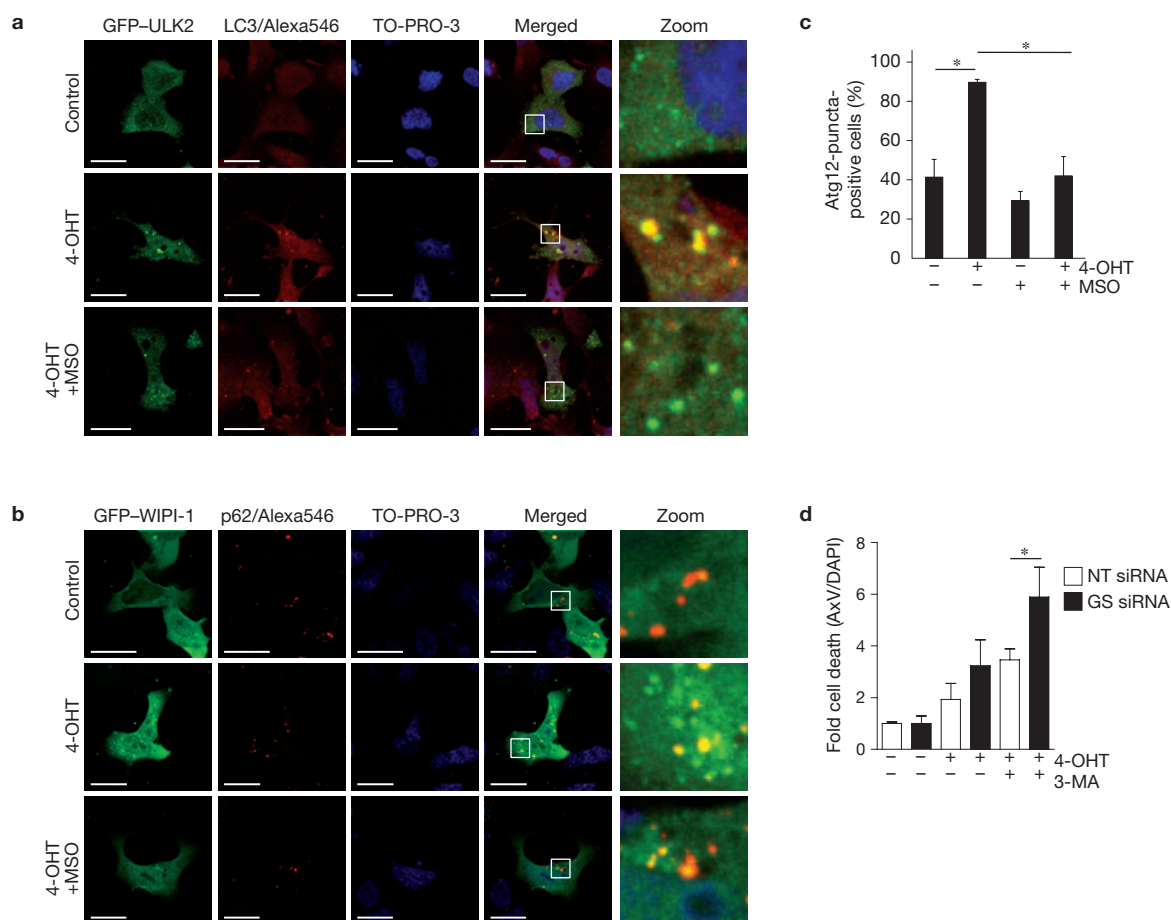


**Figure 6** FOXO-mediated glutamine synthetase activation induces autophagosome formation and increases the level of survival. **(a)** DLD1 cells expressing FOXO3(A3)-ER were transiently transfected with GFP-ULK2 and stimulated with 4-OHT and MSO for 24 h in glutamine-free DMEM containing 0.1% FCS. Cells were stained for LC3 and analysed by confocal microscopy. Shown are representative pictures ( $n = 3$ ). Scale bars, 20  $\mu\text{m}$ . **(b)** DLD1 cells expressing FOXO3(A3)-ER were transiently transfected with GFP-WIPI-1 and subsequently treated with 4-OHT in the presence or absence of MSO in glutamine-free DMEM containing 0.1% FCS. After 24 h, cells were analysed for GFP and p62 expression by confocal microscopy. Shown are representative pictures

( $n = 3$ ). Scale bar, 20  $\mu\text{m}$ . **(c)** DLD1 cells expressing FOXO3(A3)-ER were treated with 4-OHT and MSO in glutamine-free DMEM containing 0.1% FCS. After 24 h cells were analysed for endogenous Atg12 puncta formation by confocal microscopy. Shown are the mean  $\pm$  s.d. ( $n = 3$ ). \* $P < 0.05$ . **(d)** DLD1 cells expressing FOXO3(A3)-ER were transfected with glutamine synthetase (GS) siRNA or non-template (NT) control siRNA, and stimulated with 4-OHT for 24 h with or without 3-methyladenine (3-MA). Apoptosis was determined by FACS analysis after labelling cells with annexin V (AxV)-phycoerythrin and DAPI. The graph shows relative fold versus control samples, mean  $\pm$  s.e.m. ( $n = 3$ ). \* $P < 0.05$ .

in FOXO TKO MEFs, strongly supporting a causal link between FOXO activity and autophagy as a survival mechanism. Furthermore, inhibition of autophagy by 3-MA or chloroquine after conditional FOXO activation resulted in a significantly reduced level of cell viability, suggesting that the induction of autophagy by FOXO3 is important for cellular survival (Supplementary Fig. S4e).

In addition, we evaluated apoptosis in DLD1 FOXO3(A3)-ER cells transfected with a siRNA against glutamine synthetase. Activation of FOXO3 in the absence of glutamine synthetase increased the level of apoptotic cell death, which was enhanced by 3-MA, suggesting that the induction of autophagy by FOXO3-mediated upregulation of glutamine synthetase is important for cellular survival (Fig. 6d).

## DISCUSSION

By global comparative microarray analysis we have identified glutamine synthetase as a downstream effector of the PI(3)K-PKB-FOXO

signalling network. Activation of FOXO transcription factors induces glutamine synthetase expression and activity resulting in increased glutamine levels. Importantly our data reveal that this increase in glutamine levels is, at least in part, required for FOXO3-mediated induction of autophagy. This is apparently an important survival mechanism for cells, as blockade of autophagy with chemical inhibitors or reduced glutamine synthetase expression reduced the viability of FOXO3-activated cells. Functional analysis of *C. elegans* revealed that the regulation of glutamine synthetase by this pathway is also evolutionarily conserved. Taken together, these data indicate that one mechanism by which growth-factor deprivation can regulate autophagic flux is through modulation of glutamine synthetase expression.

Recently, FOXO3 has been reported to be an important regulator of autophagy during muscle atrophy by increasing the expression of several autophagy-related genes, including those encoding GABARAP1, ATG12, BNIP3 and Beclin 1 (refs 27,28). FOXO1 has also very recently

been shown to induce autophagy in JNK-deficient neurons<sup>29</sup>. In contrast, we did not find similar changes in GABARAPL1, ATG12, BNIP3 and Beclin 1 mRNA expression levels after activation of FOXO3 (Supplementary Fig. S5a), indicating FOXO-mediated induction of autophagy can apparently be regulated through both regulation of ATG-related gene expression and Atg protein employment in the process of autophagic degradation (this study) depending on the cellular context. Upregulation of these previously reported autophagy-related genes may not be responsible for the induction of autophagy *per se*, but rather to act to replenish components that are consumed during autophagic flux. This hypothesis is strengthened by the observation that their increased expression is not itself sufficient to induce autophagy<sup>27,28</sup>. However, Atg protein recruitment to pre-autophagosomal membranes provides the initial signal to form autophagosomes, and this is precisely what occurs on FOXO-mediated glutamine synthetase activation in multiple different cell lines, tested here.

In addition, FOXO1 has recently been shown to induce autophagy independently of transcription, through direct association with Atg7 (ref. 30). However, generally under conditions of growth-factor/nutrient starvation, FOXO transcription factors translocate to the nucleus and we have demonstrated that upstream activators of Atg7, such as WIPI-1, are involved in FOXO-mediated autophagy (this study). We have shown that glutamine synthetase activity is not only required for FOXO3-mediated induction of autophagy, but in addition we demonstrate that glutamine treatment alone is sufficient to increase levels of autophagy. Recently, it has been demonstrated that glutaminolysis and subsequent formation of ammonia can induce autophagy. This was achieved by keeping the cells in the same medium for more than 48 h or by depriving them of glucose<sup>31,32</sup>. FOXO-induced autophagy is a relatively rapid process allowing cells to respond quickly to growth-factor/nutrient deprivation and in our system FOXO3 activation does not result in significant changes in intracellular ammonia levels or cell swelling (Supplementary Fig. S5b–d), indicating that increased ammonia is not involved in glutamine-synthetase-induced autophagosome formation.

The precise mechanisms involved in amino-acid-mediated regulation of autophagy remain incompletely understood. Previous studies have demonstrated that the level of autophagy is regulated by the nutrient-sensing mTOR pathway<sup>18,19</sup>. mTORC1 is thought to phosphorylate and thereby inhibit the Atg1 complex, which is required for the early steps of autophagosome formation<sup>33</sup>. Amino acids can activate mTORC1 through the class III PI(3)K hVps34, but the mechanism is poorly understood<sup>16</sup>.

Recently it has been reported that activation of mTORC1 by EAAs was dependent on a bidirectional transporter, which regulates the simultaneous import of EAAs into the cell and the efflux of glutamine<sup>34</sup>. In this study, pre-loading cells with glutamine for one hour was required for amino-acid-stimulated phosphorylation of S6K. In contrast, we have shown that FOXO3 activation for 24 h decreased the level of amino-acid-induced phosphorylation of S6K in a glutamine-synthetase-dependent manner (Fig. 4a). This suggests that the effect of glutamine on mTOR signalling may have a differential outcome depending on the duration of the glutamine treatment. Furthermore, the effects of glutamine on autophagy might differ in different cell types. In liver cells, amino-acid-mediated regulation of autophagy is responsible for the rapid induction of proteolysis following starvation<sup>19,35</sup>. Stimulation

of liver cells with amino acids suppresses protein degradation, and eight regulatory amino acids, including glutamine, were found to be responsible for this response<sup>36</sup>. Suppression of proteolysis correlated with increased phosphorylation of p70S6 kinase, but the exact mechanism has not been well characterized<sup>37</sup>. However, regulation of autophagy during starvation in the liver is likely to be independent of glutamine synthetase because the expression of glutamine synthetase in the liver is limited to a small population of parenchymal cells surrounding the terminal hepatic venules<sup>38</sup>. In contrast, glutamine has been described to increase the level of autophagy as measured by LC3 cleavage in intestinal epithelial cells<sup>39</sup>, indicating that regulation of autophagy by amino acids may have distinct outcomes depending on the cell type.

AMP kinase (AMPK) is a well-described mTORC1 inhibitor and also regulator of autophagy<sup>40</sup>. To investigate whether AMPK may be required for glutamine-synthetase-mediated autophagy, we performed AMPK knockdown in DLD1 FOXO3(A3)-ER cells. As shown in Supplementary Fig. S6, knockdown of AMPK did not prevent FOXO3-induced autophagy, indicating that AMPK-mediated mTOR inhibition is probably not involved in this process. During amino-acid-mediated activation of mTOR, the Ragulator–Rag complex mediates translocation of mTOR to the lysosomal surface, which is required for its activation<sup>17</sup>. Fluorescent imaging of mTOR and LAMP2 in control cells showed that mTOR is indeed localized at lysosomes. Importantly, the mTOR–LAMP2 co-localization was abrogated after FOXO3 activation, which could be rescued by the glutamine synthetase inhibitor MSO (Fig. 4b,c). These results indicate that one mechanism by which glutamine synthetase activity inhibits mTORC1 activation is by preventing the translocation of mTOR to lysosomal surfaces. This model would explain previous observations that MSO stimulates phosphorylation of the mTORC1 substrate p70S6 kinase<sup>41</sup>.

FOXOs have been demonstrated to act as tumour suppressors, and conditional *Foxo1,3,4*<sup>-/-</sup> mice develop spontaneous lymphomas and haemangioma<sup>42</sup>. Autophagy has also been proposed to act as a tumour suppressive mechanism by protecting cells from metabolic stress and oxidative damage, thereby conferring stress tolerance, limiting damage and sustaining viability under adverse conditions (reviewed in ref. 43). Activation of oncogenic signalling pathways, such as PI(3)K and mTOR, suppresses autophagy, whereas many tumour suppressors, including PTEN and p53, lead to an induction through mTOR inhibition. We propose that the induction of autophagy by FOXO-mediated modulation of glutamine metabolism would not only allow cells to survive in the absence of nutrients, but also contribute to the tumour suppressive function of FOXOs through protection of cells from the build up of cellular damage. □

## METHODS

Methods and any associated references are available in the online version of the paper.

*Note: Supplementary Information is available in the online version of the paper*

## ACKNOWLEDGEMENTS

We thank R. Korswagen for helpful discussions. K.E.v.d.V. was supported by a grant from the Dutch Scientific Organisation (NWO-VIDI), R.G. was supported by grants (0313081F and 0315735, Virtual Liver) from the German Federal Ministry of Education and Research (BMBF), T.P.-C. was supported by the German Research Foundation (DFG; SFB 773, A03), R.v.B. was supported by a grant from CTMM and L.P.V. was supported by a grant from NIRM.

## AUTHOR CONTRIBUTIONS

K.E.v.d.V. was involved in experimental strategy and design, performed experiments, analysed data and wrote the paper. P.E., S.J.V., R.v.B., M.P., I.J.v.Z., M.M., S.Z., C.P., L.P.V., M.J.A.G.K., A.K.B. and T.B.D. performed experiments. T.P.-C., F.C.H., R.G. and B.M.B. were involved in experimental design. P.J.C. was involved in experimental strategy and design and wrote the paper.

## COMPETING FINANCIAL INTERESTS

The authors declare no competing financial interests.

Published online at [www.nature.com/doi/10.1038/ncb2536](http://www.nature.com/doi/10.1038/ncb2536)

Reprints and permissions information is available online at [www.nature.com/reprints](http://www.nature.com/reprints)

- Burgering, B. M. & Coffey, P. J. Protein kinase B (c-Akt) in phosphatidylinositol-3-OH kinase signal transduction. *Nature* **376**, 599–602 (1995).
- Stephens, L. *et al.* Protein kinase B kinases that mediate phosphatidylinositol 3,4,5-trisphosphate-dependent activation of protein kinase B. *Science* **279**, 710–714 (1998).
- Calnan, D. R. & Brunet, A. The FoxO code. *Oncogene* **27**, 2276–2288 (2008).
- Dorman, J. B., Albinder, B., Shroyer, T. & Kenyon, C. The age-1 and daf-2 genes function in a common pathway to control the lifespan of *Caenorhabditis elegans*. *Genetics* **141**, 1399–1406 (1995).
- Kimura, K. D., Tissenbaum, H. A., Liu, Y. & Ruvkun, G. daf-2, an insulin receptor-like gene that regulates longevity and diapause in *Caenorhabditis elegans*. *Science* **277**, 942–946 (1997).
- Paradis, S. & Ruvkun, G. *Caenorhabditis elegans* Akt/PKB transduces insulin receptor-like signals from AGE-1 PI3 kinase to the DAF-16 transcription factor. *Genes Dev.* **12**, 2488–2498 (1998).
- Dansen, T. B. & Burgering, B. M. Unravelling the tumor-suppressive functions of FOXO proteins. *Trends Cell Biol.* **18**, 421–429 (2008).
- Kops, G. J. *et al.* Control of cell cycle exit and entry by protein kinase B-regulated forkhead transcription factors. *Mol. Cell Biol.* **22**, 2025–2036 (2002).
- Tran, H. *et al.* DNA repair pathway stimulated by the forkhead transcription factor FOXO3a through the Gadd45 protein. *Science* **296**, 530–534 (2002).
- Delpuech, O. *et al.* Induction of Mxi1-SR alpha by FOXO3a contributes to repression of Myc-dependent gene expression. *Mol. Cell Biol.* **27**, 4917–4930 (2007).
- Mei, Y. *et al.* FOXO3a-dependent regulation of Pink1 (Park6) mediates survival signaling in response to cytokine deprivation. *Proc. Natl Acad. Sci. USA* **106**, 5153–5158 (2009).
- van der Vos, K. E. & Coffey, P. J. The extending network of FOXO transcriptional target genes. *Antioxid. Redox. Signal.* **14**, 579–592 (2010).
- Eisenberg, D., Gill, H. S., Pfluegl, G. M. & Rotstein, S. H. Structure-function relationships of glutamine synthetases. *Biochim. Biophys. Acta* **1477**, 122–145 (2000).
- Berlicki, L. Inhibitors of glutamine synthetase and their potential application in medicine. *Mini. Rev. Med. Chem.* **8**, 869–878 (2008).
- DeBerardinis, R. J. & Cheng, T. Q's next: the diverse functions of glutamine in metabolism, cell biology and cancer. *Oncogene* **29**, 313–324 (2010).
- Wullschlegel, S., Loewith, R. & Hall, M. N. TOR signaling in growth and metabolism. *Cell* **124**, 471–484 (2006).
- Sancak, Y. *et al.* Ragulator–Rag complex targets mTORC1 to the lysosomal surface and is necessary for its activation by amino acids. *Cell* **141**, 290–303 (2010).
- Blommaert, E. F., Luiken, J. J., Blommaert, P. J., van Woerkom, G. M. & Meijer, A. J. Phosphorylation of ribosomal protein S6 is inhibitory for autophagy in isolated rat hepatocytes. *J. Biol. Chem.* **270**, 2320–2326 (1995).
- Mortimore, G. E. & Schworer, C. M. Induction of autophagy by amino-acid deprivation in perfused rat liver. *Nature* **270**, 174–176 (1977).
- Kabeya, Y. *et al.* LC3, a mammalian homologue of yeast Apg8p, is localized in autophagosome membranes after processing. *EMBO J.* **19**, 5720–5728 (2000).
- Rubinsztein, D. C. *et al.* In search of an 'autophagometer'. *Autophagy* **5**, 585–589 (2009).
- Proikas-Cezanne, T., Ruckerbauer, S., Stierhof, Y. D., Berg, C. & Nordheim, A. Human WIPI-1 puncta-formation: a novel assay to assess mammalian autophagy. *FEBS Lett.* **581**, 3396–3404 (2007).
- Codogno, P., Mehrpour, M. & Proikas-Cezanne, T. Canonical and non-canonical autophagy: variations on a common theme of self-eating? *Nat. Rev. Mol. Cell Biol.* **13**, 7–12 (2011).
- Mizushima, N. & Komatsu, M. Autophagy: renovation of cells and tissues. *Cell* **147**, 728–741 (2011).
- Lum, J. J. *et al.* Growth factor regulation of autophagy and cell survival in the absence of apoptosis. *Cell* **120**, 237–248 (2005).
- Mizushima, N., Yoshimori, T. & Levine, B. Methods in mammalian autophagy research. *Cell* **140**, 313–326 (2010).
- Mammucari, C. *et al.* FoxO3 controls autophagy in skeletal muscle *in vivo*. *Cell Metab.* **6**, 458–471 (2007).
- Zhao, J. *et al.* FoxO3 coordinately activates protein degradation by the autophagic/lysosomal and proteasomal pathways in atrophying muscle cells. *Cell Metab.* **6**, 472–483 (2007).
- Xu, P., Das, M., Reilly, J. & Davis, R. J. JNK regulates FoxO-dependent autophagy in neurons. *Genes Dev.* **25**, 310–322 (2011).
- Zhao, Y. *et al.* Cytosolic FoxO1 is essential for the induction of autophagy and tumour suppressor activity. *Nat. Cell Biol.* **12**, 665–675 (2010).
- Cheong, H., Lindsten, T., Wu, J., Lu, C. & Thompson, C. B. Ammonia-induced autophagy is independent of ULK1/ULK2 kinases. *Proc. Natl Acad. Sci. USA* **108**, 11121–11126 (2011).
- Eng, C. H., Yu, K., Lucas, J., White, E. & Abraham, R. T. Ammonia derived from glutaminolysis is a diffusible regulator of autophagy. *Sci. Signal.* **3**, ra31 (2010).
- Pattingre, S., Espert, L., Biard-Piechaczyk, M. & Codogno, P. Regulation of macroautophagy by mTOR and Beclin 1 complexes. *Biochimie* **90**, 313–323 (2008).
- Nicklin, P. *et al.* Bidirectional transport of amino acids regulates mTOR and autophagy. *Cell* **136**, 521–534 (2009).
- Seglen, P. O. & Gordon, P. B. Amino acid control of autophagic sequestration and protein degradation in isolated rat hepatocytes. *J. Cell Biol.* **99**, 435–444 (1984).
- Schworer, C. M. & Mortimore, G. E. Glucagon-induced autophagy and proteolysis in rat liver: mediation by selective deprivation of intracellular amino acids. *Proc. Natl Acad. Sci. USA* **76**, 3169–3173 (1979).
- Krause, U., Bertrand, L., Maisin, L., Rosa, M. & Hue, L. Signalling pathways and combinatory effects of insulin and amino acids in isolated rat hepatocytes. *Eur. J. Biochem.* **269**, 3742–3750 (2002).
- Gebhardt, R. & Mecke, D. Heterogeneous distribution of glutamine synthetase among rat liver parenchymal cells *in situ* and in primary culture. *EMBO J.* **2**, 567–570 (1983).
- Sakiyama, T., Musch, M. W., Ropeleski, M. J., Tsubouchi, H. & Chang, E. B. Glutamine increases autophagy under Basal and stressed conditions in intestinal epithelial cells. *Gastroenterology* **136**, 924–932 (2009).
- Zhao, M. & Klionsky, D. J. AMPK-dependent phosphorylation of ULK1 induces autophagy. *Cell Metab.* **13**, 119–120 (2011).
- Tardito, S. *et al.* The non-proteinogenic amino acids L-methionine sulfoximine and DL-phenylthiothricin activate mTOR. *Amino Acids* **42**, 2507–2512 (2011).
- Paik, J. H. *et al.* FoxOs are lineage-restricted redundant tumor suppressors and regulate endothelial cell homeostasis. *Cell* **128**, 309–323 (2007).
- White, E. & DiPaola, R. S. The double-edged sword of autophagy modulation in cancer. *Clin. Cancer Res.* **15**, 5308–5316 (2009).

## METHODS

**Constructs.** SR $\alpha$ -myr110 $\alpha$ -ER, SR $\alpha$ -myrPKB-ER and pcDNA3-HA-FOXO3(A3)-ER have been described previously<sup>44,45</sup>. pcDNA3-HA-FOXO4(A3)-ER was generated by cloning FOXO4(A3) without the stop codon into pcDNA3 containing the hormone-binding domain of the oestrogen receptor (pcDNA3-ER). The pT81 and pXP2 constructs expressing the glutamine synthetase reporter have been described previously<sup>46,47</sup>. In the pXP2 construct expressing -2,520/+105 bp from the glutamine synthetase reporter, FOXO-binding sites 1–5 were mutated by quick-change mutagenesis: the core TGT sequence from the FOXO motif TTGTTTAC was mutated into ACA. Primer sequences can be found in Supplementary Table S1.

DLD1 cells expressing FOXO3(A3)-ER were transfected using Lipofectamine RNAiMAX reagents (Invitrogen) with 20 nM human *GLUL* siRNA for silencing of glutamine synthetase (Thermo Scientific, ON-TARGET plus SMARTpool, L-008228-01). The GFP-WIPI-1 and the GFP-ULK2 constructs were previously described<sup>8</sup>.

**Cell culture.** Ba/F3 cells were cultured as previously described in the presence of mouse IL-3 (ref. 49). For the generation of clonal Ba/F3 cells stably expressing myrPI(3)K-ER, myrPKB-ER, FOXO3(A3)-ER or FOXO4(A3)-ER, SR $\alpha$ -myr110 $\alpha$ -ER, SR $\alpha$ -myrPKB-ER, pcDNA3-HA-FOXO3(A3)-ER or pcDNA3-HA-FOXO4(A3)-ER were electroporated into Ba/F3 cells. Cells were maintained in the presence of 1 mg ml<sup>-1</sup> G418 (Gibco) and clonal lines were generated by limited dilution. Bone-marrow-derived MSCs were obtained from healthy volunteers and cultured in MEM- $\alpha$  (Gibco) supplemented with 10% fetal bovine serum (Hyclone), penicillin and streptomycin (Invitrogen), 1 ng ml<sup>-1</sup> basic fibroblasts growth factor (bFGF; Invitrogen), 0.2 mM L-ascorbic acid-2-phosphate (Sigma-Aldrich) and 2 mM L-glutamine (Gibco). MSCs were selected for plastic adherence. MSCs were immortalized by stable transduction of the retroviral pBabe-hygro-hTERT (human telomerase reverse transcriptase) construct and clonally expanded in selection with hygromycin B (Invitrogen). Stable expression of FOXO3(A3)-ER in MSCs, and the human osteosarcoma cell line U2OS, was performed as described above. MEFs derived from triple conditional Foxo knockout mice (Foxo1<sup>L/L</sup>: Foxo3<sup>L/L</sup>: Foxo4<sup>L/L</sup>, ref.<sup>42</sup>, a gift from J.-H. Paik, Department of Pathology, Seoul National University Bundang Hospital, Seoul National University College of Medicine, Seongnam, Republic of Korea and R. DePinho, Huffington Center On Aging and the Department of Molecular Physiology and Biophysics, Baylor College of Medicine, Houston, Texas, USA) were immortalized by viral transduction with pBabe-hygro-SV40-largeT. Clonal lines were generated by limited dilution. To ensure equal levels of large T in all cells, clonal cell lines were made by seeding single cells and were infected with Cre-recombinase-expressing adenovirus (Vector Biolabs). Subsequently cells were screened for recombination of LoxP sites for all three FoxOs by PCR with primer sets discriminating between wild-type, floxed and recombined alleles as described previously<sup>42</sup>. MEFs, DLD1, U2OS and 293 cells were cultured in DMEM containing GlutaMAX (Invitrogen), 10% fetal bovine serum and penicillin and streptomycin (Invitrogen). DLD1 cells expressing FOXO3(A3)-ER have been described previously<sup>8</sup>.

**Microarray analysis.** For microarray analysis, RNA was amplified, labelled and hybridized on Corning UltraGAPS slides containing mouse 70-base oligonucleotides (Operon, mouse V2 AROS) as previously described<sup>50</sup>. Hybridized slides were scanned on an Agilent scanner (G2565AA) at 100% laser power, 30% PMT. After data extraction using ImageGen 8.0 (BioDiscovery), print-tip Loess normalization was performed on mean spot intensities. Data were analysed using analysis of variance (ANOVA; R version 2.2.1/MAANOVA version 0.98-7; <http://www.r-project.org/>). In a fixed effect analysis, sample, array and dye effects were modelled. *P* values were determined by a permutation F2-test, in which residuals were shuffled 5,000 times globally. Genes with *P* < 0.05 after family-wise error correction (>1.7-fold) were considered significantly changed.

**Antibodies and reagents.** Antibodies against SQSTM1/p62 (D-3, sc-28359), actin (I-19, sc1616) and ER (MC-20, sc-542) were from Santa Cruz, phospho-PKB (S473, 193H12, 4058) and phospho-p70S6 kinase (Thr 389, 9,205) were from Cell Signaling Technologies, glutamine synthetase (610518) and p27 (610241) were from BD Biosciences, phospho-FOXO3 (T32, 9464) was from Upstate and LC3 was from Nanotools (5F10, 0231-100). Secondary antibodies donkey-anti-mouse-DyLight488 (715-485-150), donkey-anti-rabbit-Cy3 (711-165-152) and donkey-anti-rabbit-DyLight549 (711-505-152) were from Jackson. Tubulin antibody (T5168), glutamine, 4-OHT, MSO, 3-methyladenine, chloroquine and BafA1 were obtained from Sigma-Aldrich. Murine IL-3 was from Peprotech. LY294002 was obtained from Cayman Chemical, PKB inhibitor VIII was from Calbiochem and rapamycin was from Biomol Research. Ba/F3 cells, U2OS cells and MSCs were stimulated with 100 nM 4-OHT, and DLD cells were stimulated with 500 nM 4-OHT unless otherwise indicated. mIL-3 was used at a concentration of 5 ng ml<sup>-1</sup>, and

MSO at 1 mM unless otherwise indicated. Anti-AMPK( $\alpha$ 1/2) (2603) was obtained from Cell Signalling. Amino-acid-free medium (EBSS) was from Sigma-Aldrich and WST-1 was from Roche.

**Western blotting.** Western blot analysis was performed using standard techniques. In brief, Ba/F3 cells were lysed in Laemmli buffer (in the case of Ba/F3 cells) or SDS sample buffer. Equal amounts of proteins were analysed by SDS-polyacrylamide gel electrophoresis. Proteins were transferred to Immobilon-P and incubated with the appropriate antibodies according to the manufacturer's conditions, at a dilution of 1:1,000 or 1:500 for phospho-specific antibodies. Membranes were washed, incubated with appropriate secondary antibodies (1:10,000) and developed by ECL (Amersham Pharmacia).

**RNA isolation and quantitative rtPCR.** Cells were lysed in 1 ml TRIzol (Invitrogen) and total RNA was isolated according to the manufacturer's protocol. DNase treatment was performed using Qiagen's RNeasy kit (Qiagen). Equal amounts of RNA were reverse transcribed with SuperScript III reverse transcriptase (Invitrogen) and amplified using an Biorad Cycler with the primer pairs for mouse glutamine synthetase and normalized using B2M. Primer sequences can be found in Supplementary Table S1.

**Reporter assays.** HEK293 cells were transfected with glutamine synthetase reporter constructs together with pECE-HA-FKHRL1(A3) and Renilla to normalize for transfection efficiency using polyethylenimine. After 40 h, cells were lysed in 100  $\mu$ l passive lysis buffer and assayed for luciferase activity using the Dual-Luciferase Reporter Assay System (Promega).

**Glutamine synthetase activity assay.** Cells lysed in 50 mM imidazole and incubated at -80 °C for at least 4 h. Equal amounts of proteins were analysed for glutamine synthetase activity as previously described<sup>51</sup>. In brief, samples were mixed with  $\times$ 2 glutaminesynthetase activity buffer and incubated in a 96-well plate at 37 °C for 30 min. Next, an equal volume of glutamine synthetase stop solution was added and the absorbance at 560 nm was determined. Absorbance values of the formed product glutamyl- $\gamma$ -hydroxamate were converted to nanomoles of product by a calibration curve using commercially available glutamyl- $\gamma$ -hydroxamate.

**Determination of extracellular amino acid concentrations.** Ba/F3 cells expressing myrPI(3)K-ER, myrPKB-ER, FOXO3(A3)-ER or FOXO4(A3)-ER were stimulated as indicated, and medium samples were taken and stored at -80 °C. Concentrations of free amino acids were determined by an automated reversed phase high-performance liquid chromatography system with precolumn derivatization using the ophthalaldehyde method<sup>52</sup>.

**Apoptosis analysis.** Cells were labelled with annexin V-phycoerythrin (Alexis) and DAPI. Apoptotic and necrotic cells were then analysed using a FACScanto cytometer (BD Biosciences).

**Confocal studies.** For the analysis of mTOR, GFP-WIPI-1 and LC3 localization, cells were adhered to microscope slides and stimulated for 24 h with 4-OHT and MSO in glutamine-free DMEM containing 0.1% FCS.

For the analysis of LC3, cells were fixed in 3% paraformaldehyde (Merck) and subsequently in 100% methanol (Merck). Cells were blocked in 10% normal donkey serum (Jackson). Slides were incubated with LC3 antibody (1:100) and ER (1:100) antibody, and donkey-anti-mouse-DyLight488 and donkey-anti-rabbit-DyLight549 (1:800), and mounted in mowiol containing 3% DABCO. Slides were examined on a Zeiss LSM 710 fluorescence microscope (Oberkochen). Using ImageJ software, the number of fluorescent spots was counted after applying a fixed threshold on projected pictures, excluding objects with a size of less than 2 pixels, and divided by the number of DAPI-stained nuclei.

For mTOR analysis, cells were fixed in 3% paraformaldehyde (Merck) and permeabilized in 0.25% saponin. Cells were blocked in 10% normal donkey serum (Jackson) and 0.25% saponin. Next, cells were incubated with mTOR antibody (Cell Signaling, 2983, clone 7C10, 1:100) and LAMP2 antibody (BD Pharmingen, 555803, 1:150), followed by donkey-anti-mouse-DyLight-488 (1:500) and donkey-anti-rabbit-Cy3 (1:500) and DAPI and mounted in mowiol containing 3% DABCO. Images were analysed and the percentage of co-localized pixels was calculated using ZEN 2009 software from Zeiss.

For the analysis of GFP-WIPI-1 puncta, DLD1 cells expressing FOXO3(A3)-ER were transiently transfected with GFP-WIPI-1. The percentage of cells positive for GFP-WIPI-1 puncta was analysed as previously described<sup>22</sup>.

For co-localization experiments of various autophagy proteins, DLD1 cells expressing FOXO3(A3)-ER were transiently transfected with GFP-WIPI-1 or GFP-ULK2. Cells were fixed with paraformaldehyde (3.7%) and prepared for indirect immunofluorescence analysis. GFP-ULK2-transfected DL23 cells were stained

with LC3 antibody (1:50) followed by anti-mouse-IgG-546 (Molecular Probes, A11003, 1:200). GFP-WIPI-1-transfected cells were stained with Atg12 (Abgent, AP1816a, 1:25) or p62 (Santa Cruz, sc28359, 1:50) followed by anti-mouse-IgG-546 or anti-rabbit-IgG-546 (1:200), respectively (Molecular Probes, A11010). TO-PRO-3 (Invitrogen, T3605) was used for nuclei staining.

**FACS analysis.** Cells were labelled with propidium iodide (Alexis) and analysed using a FACScanto cytometer (BD Biosciences). The FSC-H was analysed in cells negative for propidium iodide.

**Ammonia measurements.** The intracellular ammonia concentration in DLD1 cells was measured using the ammonia assay kit from Sigma-Aldrich (AA0100). In short, DLD1 cells expressing FOXO3(A3)-ER were stimulated with 4-OHT and MSO for 24 h in glutamine-free DMEM containing 0.1% FCS.

**Knockdown of AMPK.** Control siRNA and human *AMPK $\alpha$ 1/2* siRNA were purchased from Santa Cruz Biotechnology (sc37007 and sc45312). The human *AMPK $\alpha$ 1/2* siRNA consists of a pool of the following 3 siRNAs: sc-45312A: sense: 5'-GAUGUCAGAUGGUGAAUUtt-3', antisense: 5'-AAAUUC-ACCAUCUGACAUCtt-3'; sc-45312B: sense: 5'-CCACUGCAAUACAAUUGAtt-3', antisense: 5'-UCAAUUAGUAUUGCAGUGGtt-3'; sc-45312C: sense: 5'-CUACUGGAUUCCGUAGUAtt-3', antisense: 5'-UACUACGGAAUCCAG-UAGtt-3'.

**C. elegans assays.** Nematode strains were cultured at 20 °C using standard conditions as described previously<sup>53,54</sup>. Mutant strains used in this study were *daf-16* (*mu86*; ref 55) and *daf-2*. To measure glutamine synthetase activity, strains were synchronized to L1 by hypochlorite treatment and were placed on nematode growth medium agar plates. After 5 days, worms were lysed in 50 mM imidazole and incubated at -80 °C for at least 4 h. Lysates were thawed on ice, ground in liquid nitrogen and glutamine synthetase activity was determined as described.

**Chromatin immunoprecipitation.** Cells were crosslinked with 2 mM disuccinimidyl glutarate (Thermo Fisher Scientific) and 1% formaldehyde, and nuclei were isolated in 10 mM Tris-HCl at pH 7.5, 10 mM NaCl, 3 mM MgCl<sub>2</sub> and 0.5% NP-40 and lysed in pre-immunoprecipitation buffer (10 mM Tris-HCl pH 7.5, 10 mM NaCl, 3 mM MgCl<sub>2</sub>, 1 mM CaCl<sub>2</sub>, 4% NP-40). Lysates were sonicated and precleared with protein-A-agarose beads, followed by incubation with 5 µg antibody against FOXO3 (Millipore, 07-702) or an IgG control (Jackson, 011-000-002). Samples were washed and incubated with elution buffer (0.1 M NaHCO<sub>3</sub>, 1% SDS). Crosslinks

were reversed by adding NaCl and incubation overnight at 65 °C. Next, samples were incubated with proteinase K. rtPCR was then performed on the purified DNA.

**Statistical analysis.** Data are expressed as the mean  $\pm$  s.e.m.. Significant differences between mean values were evaluated using one-way ANOVA followed by Dunnett's test (for serial analysis of one variable) or two-way ANOVA followed by Bonferroni's post-tests (for serial analysis of two variables). \**P* < 0.05 and \*\**P* < 0.01.

Microarray data have been submitted to the GEO data repository <http://www.ncbi.nlm.nih.gov/geo/> with the following accession number: GSE35705.

44. Dijkers, P. F., Medema, R. H., Lammers, J. W., Koenderman, L. & Coffey, P. J. Expression of the pro-apoptotic Bcl-2 family member Bim is regulated by the forkhead transcription factor FKHR-L1. *Curr. Biol.* **10**, 1201–1204 (2000).
45. Dijkers, P. F. *et al.* Forkhead transcription factor FKHR-L1 modulates cytokine-dependent transcriptional regulation of p27(KIP1). *Mol. Cell Biol.* **20**, 9138–9148 (2000).
46. Fahrner, J. *et al.* Identification and functional characterization of regulatory elements of the glutamine synthetase gene from rat liver. *Eur. J. Biochem.* **213**, 1067–1073 (1993).
47. Gaunitz, F., Weber, S., Scheja, L. & Gebhardt, R. Identification of a cis-acting element and a novel trans-acting factor of the glutamine synthetase gene in liver cells. *Biochem. Biophys. Res. Commun.* **284**, 377–383 (2001).
48. Pfisterer, S. G., Mauthe, M., Codogno, P. & Proikas-Cezanne, T. Ca<sup>2+</sup>/calmodulin-dependent kinase (CaMK) signaling via CaMKI and AMP-activated protein kinase contributes to the regulation of WIPI-1 at the onset of autophagy. *Mol. Pharmacol.* **80**, 1066–1075 (2011).
49. Caldenhoven, E. *et al.* Activation of the STAT3/acute phase response factor transcription factor by interleukin-5. *J. Biol. Chem.* **270**, 25778–25784 (1995).
50. Raaben, M. *et al.* Improved microarray gene expression profiling of virus-infected cells after removal of viral RNA. *BMC Genom.* **9**, 221 (2008).
51. Deuel, T. F., Louie, M. & Lerner, A. Glutamine synthetase from rat liver. Purification, properties, and preparation of specific antisera. *J. Biol. Chem.* **253**, 6111–6118 (1978).
52. Guthke, R. *et al.* Dynamics of amino acid metabolism of primary human liver cells in 3D bioreactors. *Bioprocess. Biosyst. Eng.* **28**, 331–340 (2006).
53. Brenner, S. The genetics of *Caenorhabditis elegans*. *Genetics* **77**, 71–94 (1974).
54. Lewis, J. A. & Fleming, J. T. Basic culture methods. *Methods Cell Biol.* **48**, 3–29 (1995).
55. Lin, K., Dorman, J. B., Rodan, A. & Kenyon, C. *daf-16*: an HNF-3/forkhead family member that can function to double the life-span of *Caenorhabditis elegans*. *Science* **278**, 1319–1322 (1997).

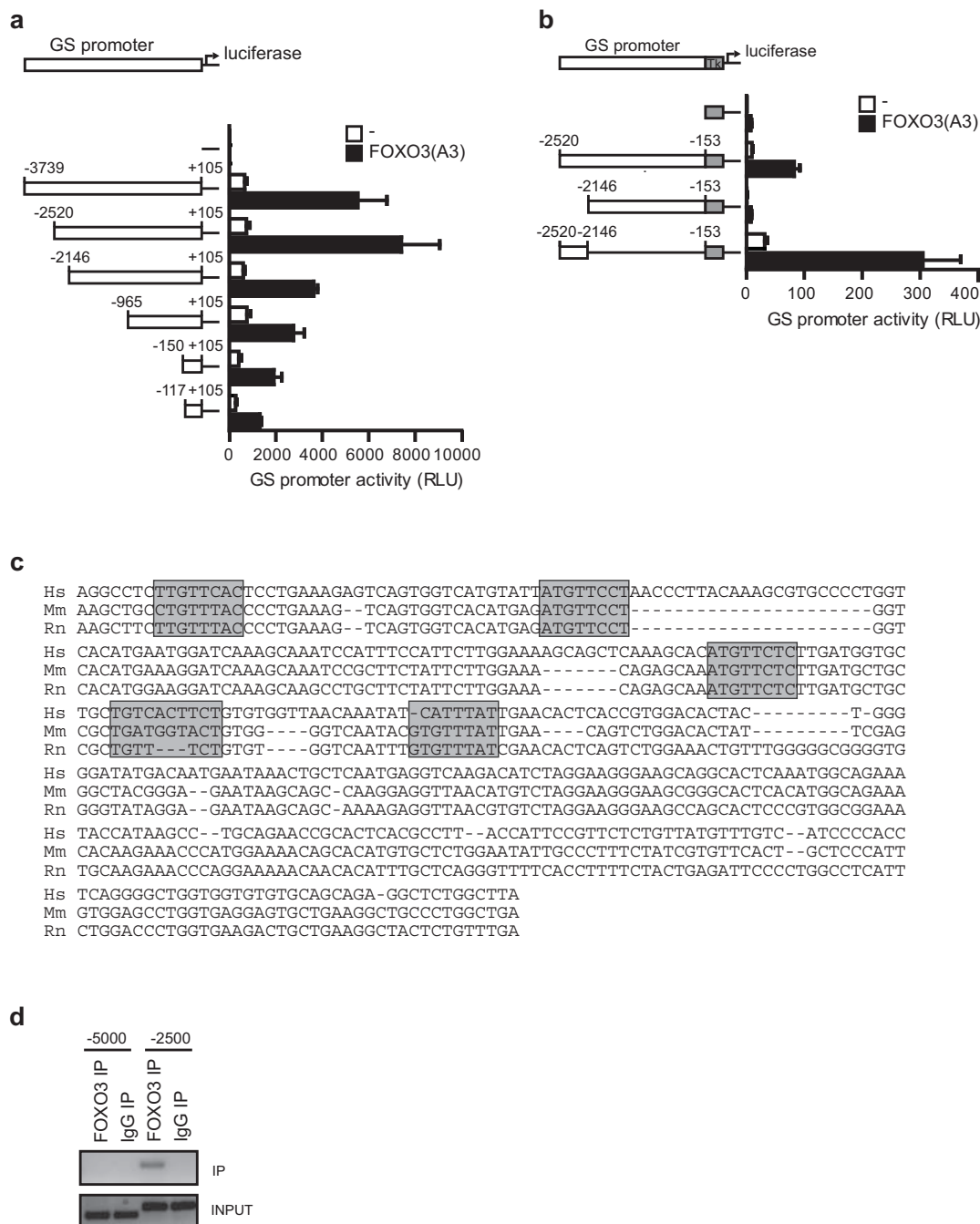


**Figure S1** FOXO3 upregulates glutamine synthetase expression through a conserved FOXO binding site in the glutamine synthetase promoter. **(a,b)** GS reporter plasmids expressing the glutamine synthetase promoter linked to a minimal Tk promoter and a luciferase gene **(a)**, or expressing different lengths of the glutamine synthetase promoter linked to a luciferase gene **(b)**, were transfected in HEK 293 cells together with Renilla and FOXO3(A3) as indicated. Luciferase activity was measured 40 hours after transfection. Data are depicted as relative luciferase units (RLU) compared to control. Shown are mean  $\pm$  SEM values (n=3). **(c)** Alignment

of putative FOXO-responsive GS promoter enhancer elements (-2520/-2146) from human, mouse and rat showing the presence of five conserved FOXO binding sites (in boxes) TTGTTTAC **(d)** 293 Cells were stimulated with LY294002 for 24 hours and chromatin immunoprecipitations were performed. Protein-DNA complexes were formaldehyde-cross-linked and chromatin fragments from these cells were subjected to immunoprecipitation with a control antibody or antibodies to FOXO3a as indicated. After cross-link reversal, the co-immunoprecipitated DNA was amplified by RT-PCR and resolved on an agarose gel.

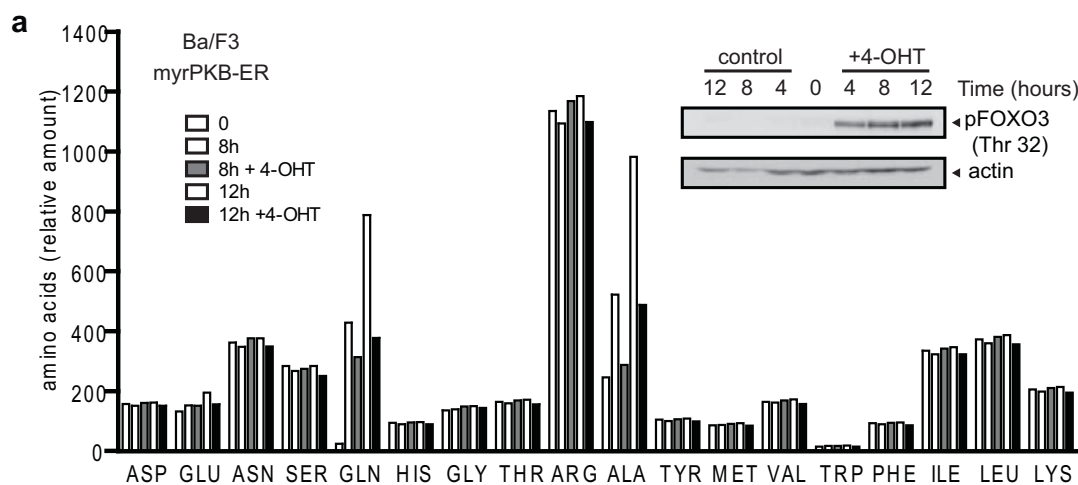


**Figure S2** Activation of PKB results in regulation of glutamine levels. Ba/F3 cells expressing myrPKB-ER were cytokine starved overnight. The next day cells were washed in PBS and put in medium without serum with or without 4OHT. At the times indicated, medium samples were taken and analysed for

amino acid levels by HPLC. In addition, cells were lysed and equal amounts of protein were analysed by western blotting for levels of phospho-FOXO3 (T32), and actin. Shown are the mean of relative amino acid levels compared to t=0 (n=2) and representative blots of these experiments.

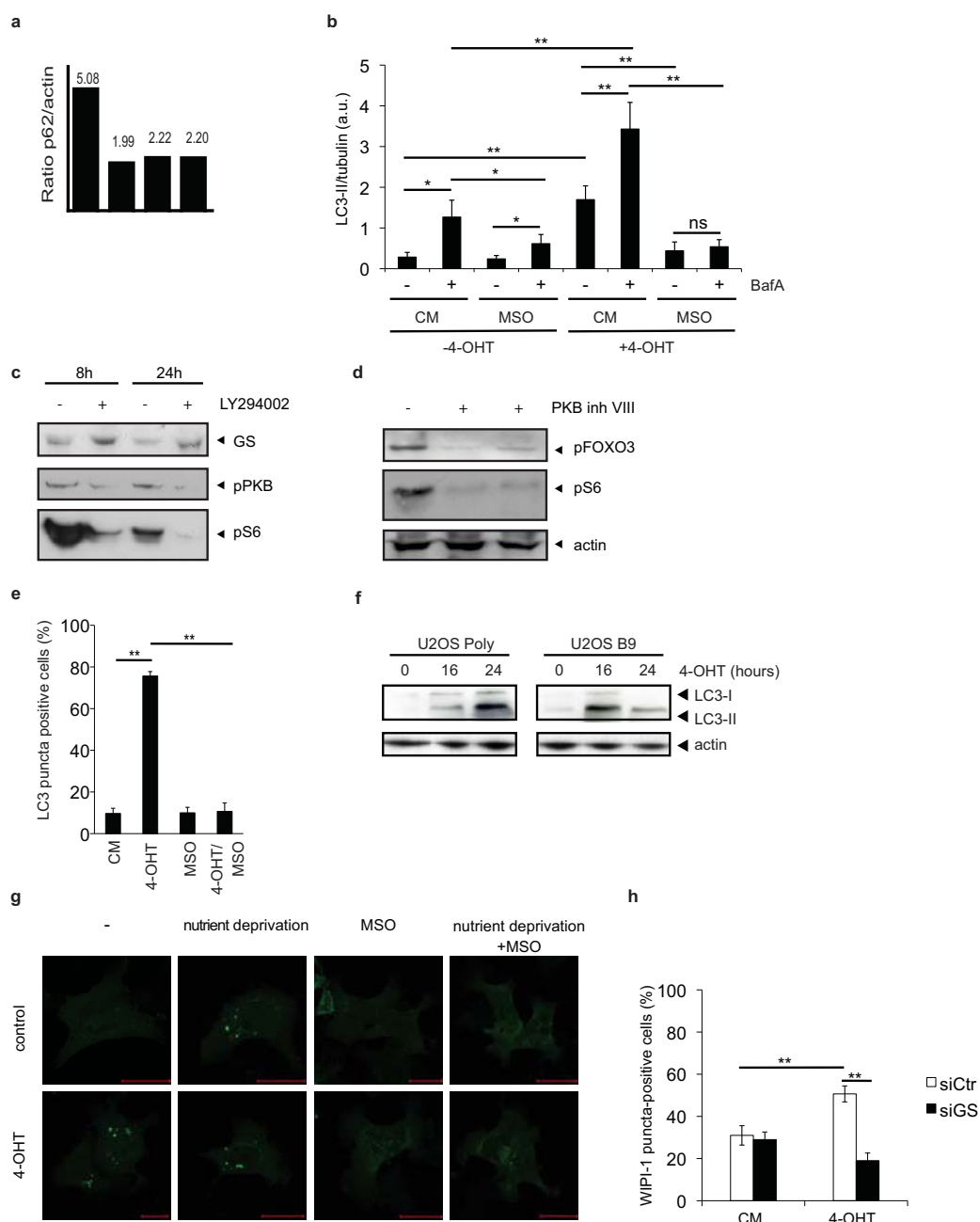


**Figure S3** FOXO3 induces autophagy through upregulation of GS activity. Quantification of Western blots shown in Figure 4f. DLD1 cells expressing FOXO3(A3)-ER were transfected with GS siRNA or non-template (NT) control siRNA and stimulated with 4-OHT for 16 hours. Cells were lysed and equal amount of proteins were analysed for levels of p62 or GS. Graph shows the ratio of p62/actin in each sample. **(b)** Quantification of Western blots shown in Figure 5a. DLD1 cells expressing FOXO3(A3)-ER were treated with or without 4OHT, MSO and Bafilomycin A. After 24 hours cells were lysed and analysed for levels of LC3 and tubulin expression. Ratio of LC3-II/tubulin was quantified using ImageJ (n=4). Shown are mean  $\pm$  SD, \*  $p < 0.05$  and \*\*  $p < 0.01$  **(c)** DLD1 cells were stimulated with LY294002 for 24 hours. Cell lysates were analysed for protein levels of GS, pPKB (S473) and pS6. **(d)** DLD1 cells were stimulated with PKB inhibitor VIII for 24 hours. Cell lysates were analysed for protein levels of pFOXO3 (T32), pS6 and actin. **(e)** DLD1 cells expressing FOXO3(A3)-ER were treated with 4OHT and MSO in DMEM without glutamine containing

0.1% FCS. After 24 hours cells were analysed for endogenous LC3 puncta formation by confocal microscopy. Shown are the mean  $\pm$  SD (n=3). \*\*  $p < 0.01$  **(f)** The osteosarcoma cell line U2OS expressing FOXO(A3)-ER was stimulated with 4OHT as indicated, cells were lysed and equal amounts of proteins were analysed for levels of LC3 and actin. **(g)** DLD1 cells expressing FOXO3(A3)-ER were transiently transfected with GFP-WIPI-1 and subsequently treated with 4OHT in the presence of absence of MSO in DMEM without glutamine containing 0.1% FCS, or medium without amino acids for 24 hours. Cells were analysed for GFP-WIPI-1 puncta formation by confocal microscopy. Shown are representative pictures corresponding to Fig. 5g (n=4). Scale bars are 20  $\mu$ m **(h)** DLD1 cells expressing FOXO3(A3)-ER were transiently transfected with GFP-WIPI-1 and GS siRNA or non-template (NT) control siRNA and subsequently treated with 4OHT in DMEM without glutamine containing 0.1% FCS. After 24 hours cells were analysed for GFP-WIPI-1 puncta formation by confocal microscopy. Shown are the mean  $\pm$  SD (n=3). \*\*  $p < 0.01$



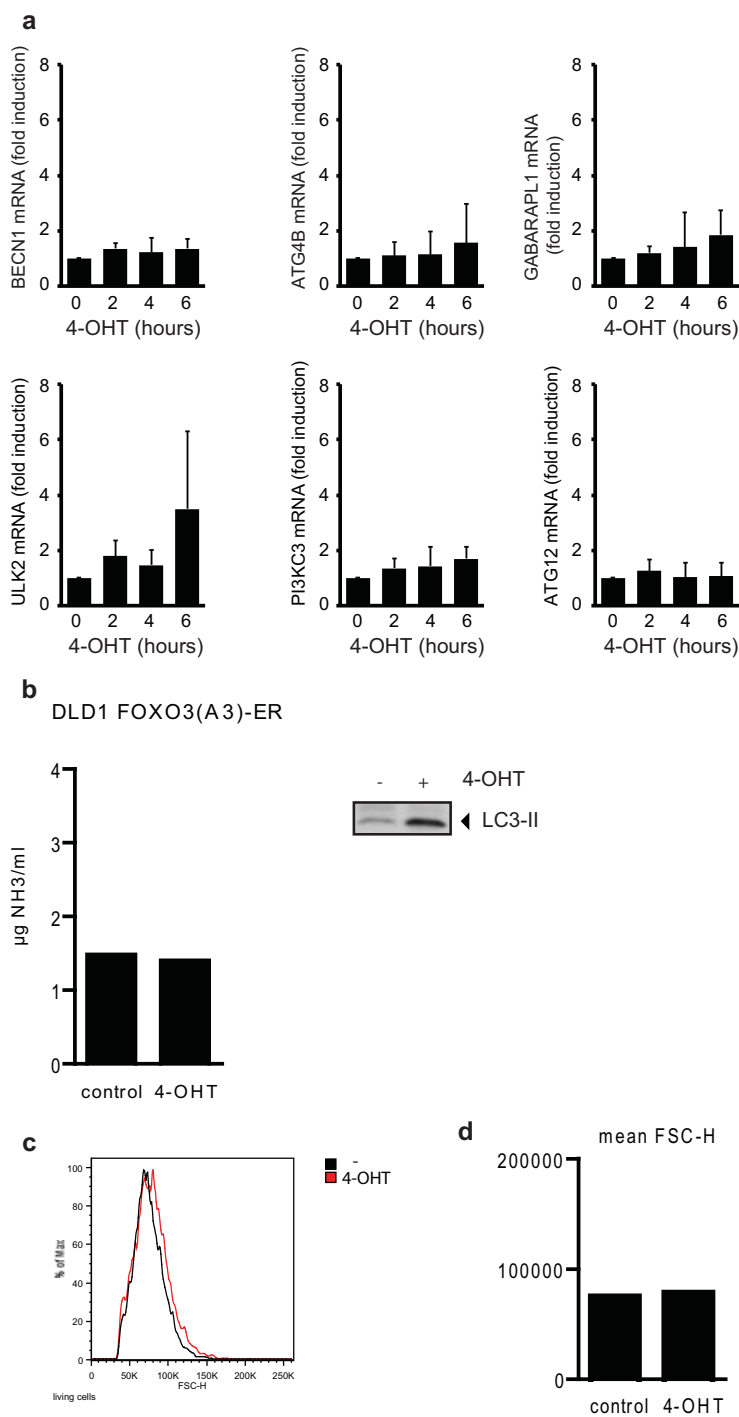


**Figure S5** Activation of FOXO3 does not affect mRNA levels of multiple autophagic markers and does not affect ammonia levels. **(a)** DLD1 cells expressing FOXO3(A3)-ER were cytokine starved overnight and stimulated with 4OHT. Relative mRNA levels of BECN1, ATG4B, GABARAPL1, ULK2, PI3KC3 and ATG12 were analysed using quantitative RT-PCR. Data are represented as mean  $\pm$  SEM values normalized for GAPDH (n=3). **(b)** DLD1 cells expressing FOXO3(A3)-ER were stimulated with 4OHT in DMEM without glutamine containing 0.1% FCS. After 24 hours supernatant was

harvested and ammonia levels were analysed. Cells were lysed and equal amounts of proteins were analysed by western blotting for levels of LC3. The graph shows the mean  $\pm$  SEM of one experiment with triplicates. **(c,d)** DLD1 cells expressing FOXO3(A3)-ER were stimulated with 4OHT in glutamine free DMEM containing 0.1% FBS. After 24 hours cells were stained with propidium iodide (PI) and analysed by flow-cytometry. Shown are histograms depicting the FSC-H of the PI-negative cells and a graph depicting the mean FSC-H. (n=1).

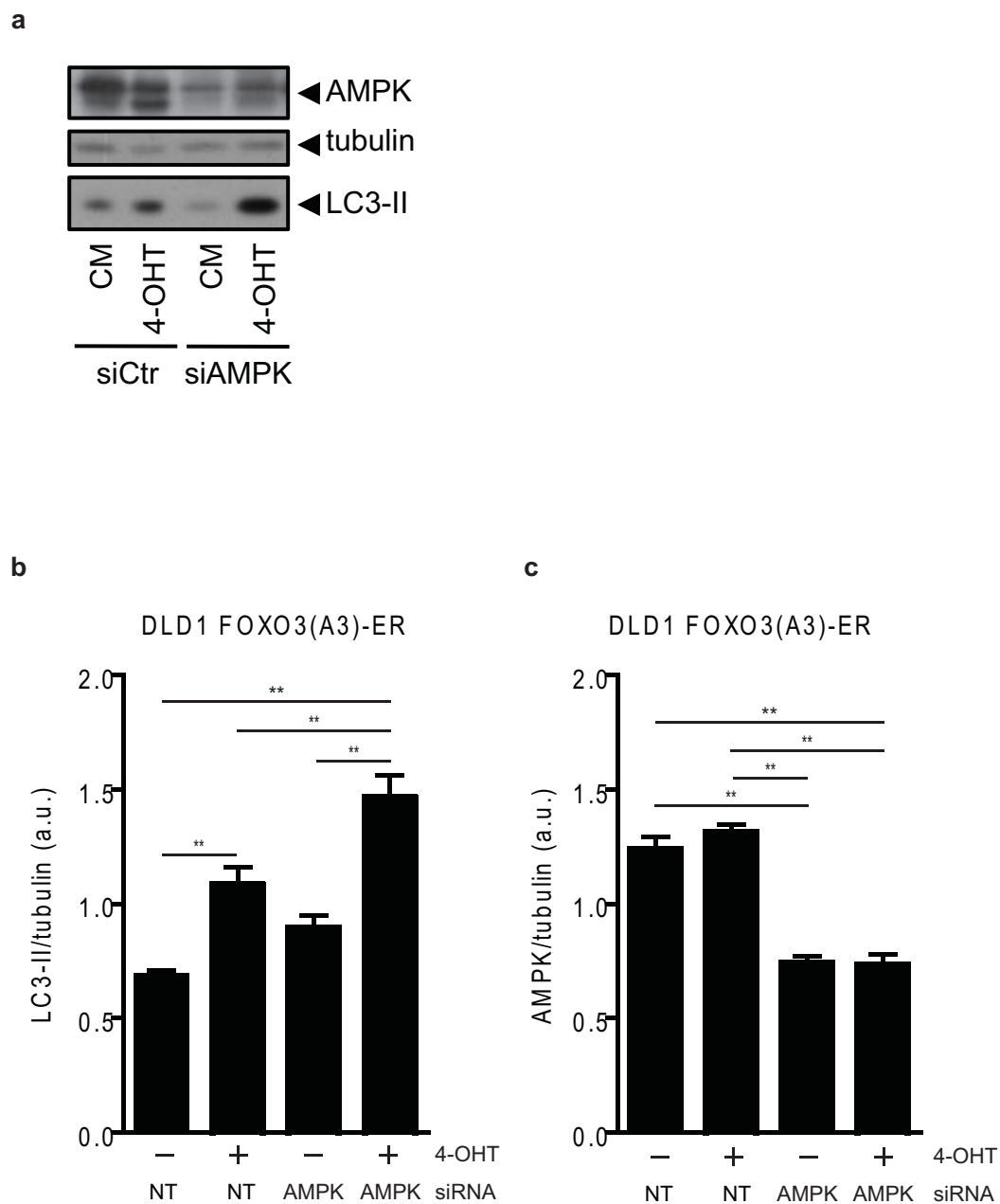


**Figure S6** FOXO-induced autophagy is not dependent on AMPK. **(a,b,c)** DLD1 cells expressing FOXO3(A3)-ER transfected with 50nM control siRNA or AMPK $\alpha$ 1/2 siRNA and stimulated with 4OHT in glutamine free DMEM containing 0.1% FBS. After 24 hours cell lysates were

analysed for protein levels of AMPK, LC3 and tubulin. **(a)** shown are representative blots (n=8) **(b,c)** Ratio of LC3-II/tubulin **(b)** and AMPK/LC3 **(c)** were quantified using ImageJ (n=8). Shown are mean  $\pm$ SD, \*\* p < 0.01.

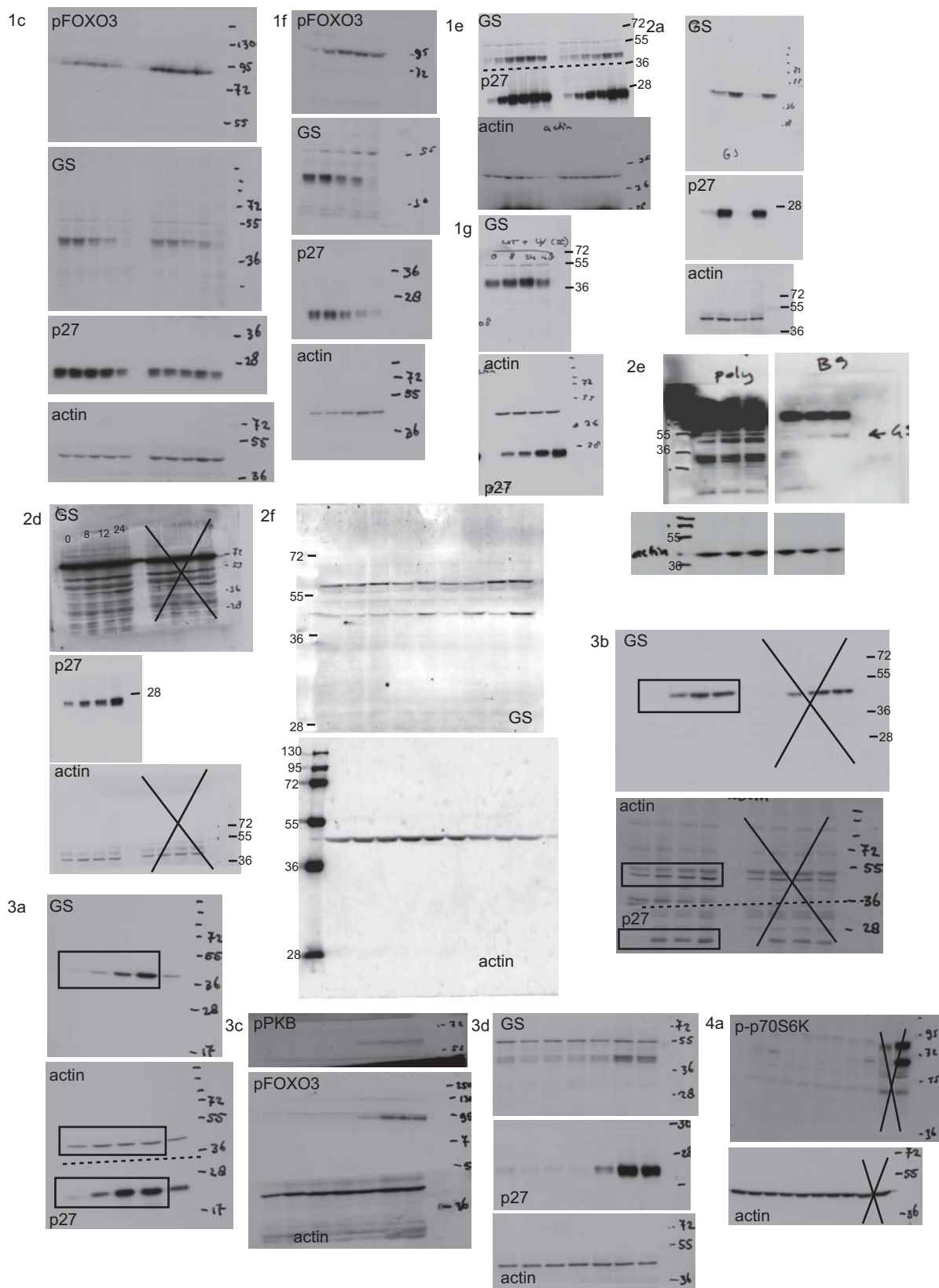


Figure S7 Full scans of western blots (Figs 1–4a).

SUPPLEMENTARY INFORMATION

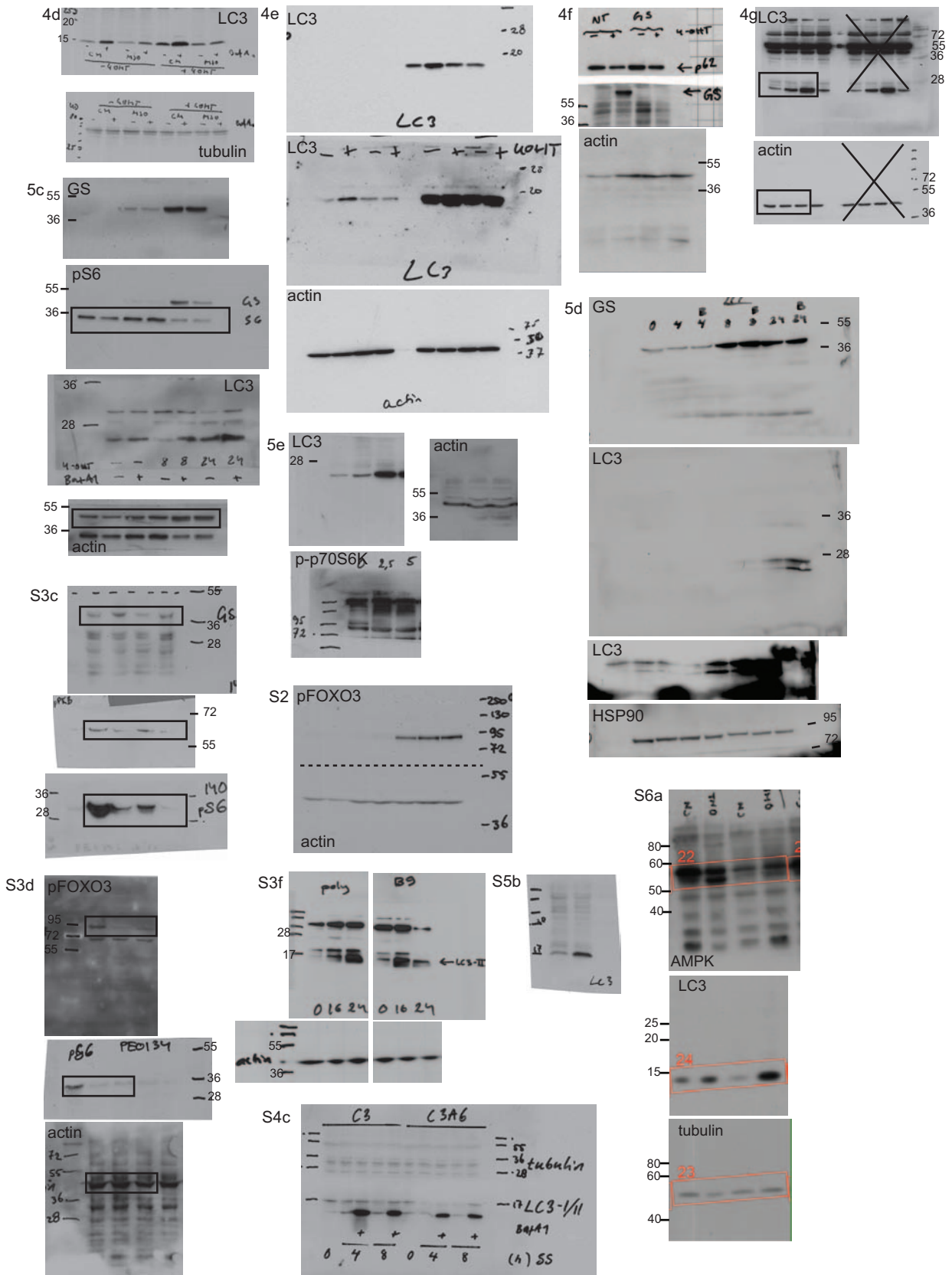


Figure S8 Full scans of western blots (Figs 4d-S6).

**Table S1** Primers used in this study. Sequences of primers used for RT-PCR and CHIP analyses, as well as GS promoter mutagenesis, are provided.